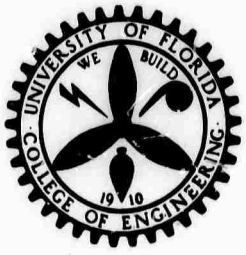

ENGINEERING AND INDUSTRIAL EXPERIMENT STATION

College of Engineering

University of Florida

Gainesville

MISSING PAGE
NUMBERS ARE BLANK
AND WERE NOT
FILMED

STRUCTURE, PROPERTIES AND RADIATION SENSITIVITY OF ELECTRICALLY BISTABLE MATERIALS

Technical Report No. 2
6 February 1971

First Annual Report
(ARPA DAHC04-70-C-0024)

ARPA Order Number:	1562
Program Code Number:	OD10
Name of Contractor:	University of Florida
Effective Date of Contract:	6 February 1970
Contract Expiration Date:	6 February 1972
Amount of Contract:	$57,816
Contract Number:	DAHC04-70-C-0024
Principal Investigator:	Dr. Derek B. Dove, telephone 904-392-1497
Project Scientist: (Technical Coordinator)	Dr. Charles Boghosian, AROD, telephone 919-286-2285

Submitted by

D. B. Dove, L. L. Hench,
R. W. Gould and R. E. Loehman
Department of Metallurgical and Materials Engineering
University of Florida
Gainesville, Florida 32601

TABLE OF CONTENTS

STRUCTURE, PROPERTIES AND RADIATION SENSITIVITY OF ELECTRICALLY BISTABLE MATERIALS

Abstract

This report describes work carried out during the first twelve months on a project directed towards a thorough electrical and metallurgical characterization of selected amorphous semiconducting materials.

A range of semiconductors of compositions Ge_xSe_{1-x} and Ge_xTe_{1-x} have been prepared and have been examined by x-ray diffraction to verify the composition limits of the glass forming regions reported by previous workers. Thin films have been prepared by flash evaporation of crushed bulk compounds and have been subjected to rdf analysis and electron microscopy, and several structural models are compared. Studies on the crystallization kinetics of the glasses are being carried out with particular reference to material composition. An interpretation of these initial experiments is given in terms of a possible structural model for the glasses.

The importance of crystallite size on fast neutron damage threshold in heterogeneous amorphous semiconductors is emphasized and the results of radiation experiments on vanadate glasses are discussed.

Table 1

Composition of Bulk Compounds Prepared

Sample	X-ray Analysis
$GeSe_2$ I	non-crystalline
$GeSe_2$ II	non-crystalline
$GeSe_2$ III	non-crystalline
$GeSe_2$ IV	non-crystalline
$GeSe_2$ V	non-crystalline
$GeSe_2$ VI	non-crystalline
GeSe I	crystalline
$GeSe_3$ I	crystalline
$GeSe_3$ II	
$GeSe_4$ I	
$GeSe_4$ II	
$GeTe_4$ I	crystalline
$GeTe_4$ III	crystalline
$GeTe_5$	crystalline
$GeTe_{5.5}$	crystalline
$Ge_{.75}As_{.25}Te_4$	non-crystalline
GeTeSe	
$Ge_{.75}As_{.25}Se_4$	
$GeSe_{1.95}As_{.05}$	
$GeSe_{2.9}As_{.1}$	
$GeSe_{.98}Te_{.98}As_{.04}$	

rate. In fact, Takamori, Roy and McCarthy[1] obtained glasses of water-quenched bulk $GeTe_x$ in the range $4.0 \leq X \leq 5.7$, while samples of similar composition in the present study proved to be crystalline. However, Takamori and coworkers' samples were considerably smaller (1 to 3 g.) than those reported here and therefore must have realized considerably higher cooling rates. We have introduced a procedure employing flattened ampoules, whereby higher quenching rates may be achieved without sacrificing sample size.

The relatively large diameter of the vycor ampoules used here (13 mm) leads to a steep gradient in cooling rates across the radius of the sample. For some materials a composition gradient was apparent to the eye; tiny crystallites were evident some distance from the surface of the sample with grain size increasing toward the interior. Takamori, Roy and McCarthy report SEM studies on $GeTe_x$ which show this effect. Similar studies on the samples reported here are in progress.

Thin films have been prepared from many of these samples by flash evaporation of powdered material from molybdenum boats held at high temperature. Thickness was measured by quartz oscillator thickness monitor. The density of some films was determined by combining thickness obtained by inteferometric techniques with mass per unit area measured by the change in frequency of the quartz plate

---

[1] T. Takamori, R. Roy and G. J. McCarthy, Matl. Res. Bull., 5, 529 (1970).

oscillator. Substrates used include glass slides, mica, rock salts and infra-red transmitting materials.

II. STRUCTURE OF THE CHALCOGENIDE BINARY GLASSES

Two binary systems have been chosen for initial systematic investigations, these being Ge_xSe_{1-x} and Ge_xTe_{1-x}. Of particular interest are the compositions GeSe, GeTe and $GeSe_2$, $GeTe_2$ since these are structural analogues of the well studied materials SiO and SiO_2. Furthermore, well defined crystal structures exist at the compositions GeSe, GeTe and $GeSe_2$, although a crystalline form of $GeTe_2$ appears not to have been reported.

Work on these systems is proceeding along three major lines,

i) radial distribution analysis of the local atomic order,

ii) electron microscopy of the microstructure, and

iii) kinetics of crystallization due to heat treatment.

In the semiannual report it was noted that the rdfs of GeTe and GeSe indicated a major difference between the local order in the glasses and in the isocompositional crystalline forms. The difference showed up in the nearest neighbor distance indicated by the rdfs (the n.n. distance is probably by far the most reliable information provided by the rdf). This nearest neighbor distance changes only slightly with composition as noted for Ge-Te alloys by Bienenstock and collaborators.[2]

---

[2] F. Betts, A. Bienenstock and S. R. Ovshinsky, N. Non-Cryst. Solids, Proc. 3rd Int. Conf. on Amorphous Semiconductors.

The problem is therefore one of describing the structure of the glass using a model that is consistent with the experimental radial distribution curves and with the observed crystallization behavior (to be described shortly).

Radial Distribution Analysis of Binary Alloys

As pointed out by several workers (for example, C. J. Pings and J. Waser[3]), the rdf analysis of intensity data from compounds may be carried out by the usual Fourier transform techniques. The data I(s) is normalized by a function denoted here by $F^2(s)$, where typically $F^2 = xf_1^2 + (1-x) f_2^2$; f_1, f_2 are the atomic scattering factors for Ge and Se (or Te) in the present case, and x is the proportion of Ge in a Ge_xSe_{1-x} compound.

It may be shown that, to a good approximation

$$\int_{-\infty}^{\infty} s\left[\frac{I(s)}{F^2} - \frac{xf_1^2 + (1-x)f_2^2}{F^2}\right] \sin(2\pi rs)ds = rA_{11}p_{11}(r)$$

$$+ rA_{12}p_{12}(r) + rA_{21}p_{21}(r) + A_{22}p_{22}(r)$$

$$- rp_0[xf_1(0) + (1-x)f_2(0)]^2/F^2(0)$$

$$= r\rho'(r) - r\rho_0'$$

The integration on the left hand side of the above equation

---

[3] C. J. Pings and J. Waser, J. Chem. Phys., 48, 3016 (1968).

is evaluated numerically for a series of values of r, the interatomic separation, and a curve of $r[\rho'(r)-\rho_0']$ is obtained which consists of a sum of distributions ρ_{ij} weighted by factors A_{ij} where $A_{ij} = f_i(0)f_j(0)/F^2(0)$; $\rho_{ij}(r)$ gives the density of atoms of type j at distance r from an atom of type i. More generally, the peaks of $\rho'(r)$ are convoluted with the transforms of the $f_i f_j/F^2$ functions.

Unfortunately, the diffraction experiment yields only $r[\rho'(r)-\rho_0']$ and not the individual $\rho_{ij}(r)$ terms, although the A_{ij} constants may be readily calculated. The breakdown of $\rho'(r)$ into $\rho_{ij}(r)$ terms is far from unique and appeal must be made to further experimentation to assist in building up a conceptual model for the structure.

Thin films of less than 200 Å in thickness were deposited onto rocksalt substrates at room temperature. The films were floated off under water and picked up on 1,000 mesh copper screening, for examination by electron microscopy and electron diffraction. A number of films were found to contain small crystallites as deposited. Other films crystallized very readily inside the diffraction camera and it was found necessary to reduce beam intensity considerably to avoid beam heating effects. Glassy films of GeTe, $GeTe_2$, $GeTe_4$ and GeSe, $GeSe_2$, $GeSe_4$ and other compositions were examined by scanning electron diffraction. In this apparatus the diffraction pattern is scanned across a detector and an electrostatic filter rejects inelastically scattered electrons. In this way in intensity profile

across the diffuse diffraction halos is obtained electrically, with experimental rejection of unwanted background intensity,[4,5]

The results of rdf measurements on GeSe are shown in Fig. 1, where a,b,c show plots of intensity vs. s, and $r[\rho'(r)-\rho_0]$ and $4\pi r^2[\rho'(r)-\rho_0']$ vs. r, respectively; s is the scattering parameter $2\sin\theta/\lambda$, where 2θ is the angle of scatter and λ is the electron de Broglie wavelength. The results for $GeSe_2$ are shown in Fig. 2. The results for $GeTe_2$ and $GeTe_4$ are shown in Figs. 4 and 5. Results for GeTe were presented in a previous report.

The three curves in the $GeTe_2$ sequence and the two curves in the $GeTe_4$ sequence show the considerable run to run variation presently occurring with these materials. It is not known whether this is a genuine structural effect since the films respond very readily to thermal treatment or whether this is due to unanticipated compositional fluctuations from run to run. These films were made by flash evaporation from crushed glass from one melt in each case. The data shown in the several rdf curves are summarized in Table 2.

Discussion of the rdfs

The nearest neighbor distance indicated by the rdf is approximately 2.42 Å for GeSe and 2.65 Å for GeTe. This

---

[4] C. W. B. Grigson, Rev. Sci. Instr., 36, 1587 (1965).

[5] D. B. Dove and P. N. Denbigh, Rev. Sci. Instr., 37, 1687 (1966).

Table 2

Summary of rdf Data

Material	Area of 1st peak	Prominent bond lengths				
GeSe	~3.0	2.42	4.10	5.0	6.1	7.85
$GeSe_2$	~3.0	2.50	4.35	5.0	6.45	8.35
GeTe	~3.8	2.65	4.25	5.0	6.3	7.6
"$GeTe_2$"	~2.2	2.55	4.00	5.10	6.00	7.5
	~2.8	2.65	4.20	5.15	6.35	8.1
	~3.7	2.65	4.45	5.10	6.70	
$GeTe_4$	~3.3	2.62	4.40	5.05	6.60	8.60
	~3.7	2.62	4.40		6.60	8.60

distance changes very slightly with composition and is only very slightly larger than the sum of the covalent radii. Figure 5a shows a plot of the ionic radii listed for Ge, Se and Te ions as listed by Pauling.[6] It is of interest to examine the variation in interatomic distance with ionicity. In Fig. 5b is shown a plot of the sum of the radii from $Ge^{4+}Te^{2-}$ to $Ge^{2+}Te^{1-}$ and to covalent GeTe. This distance changes only a little with ionicity and is close to the observed value. In contrast, the $Ge^{2+}Te^{2-}$ and $Ge^{1+}Te^{1-}$ distances are appreciably larger as reflected in the 3.0 Å separation in the crystalline GeTe rocksalt structure, although it must be noted that the ionic bond length decreases as coordination decreases. The electronegativity difference between Si and O strongly favors the formation of SiO_4 tetrahedra in silica; the electronegativity difference is much smaller in Ge-Se and smaller yet in Ge-Te glasses. Superficially, no evidence is found for residual distorted rocksalt coordination with accompanying expanded interatomic distance in either the Ge-Te or Ge-Se binary compounds. A detailed study of the rdfs is currently in progress.

It is of interest to examine how the area under the first peak in the rdf might vary with composition for three extreme models, namely

i) random mixing of four coordinated Ge and two coordinated Se (or Te) (this is one of the cases discussed by Bienenstock and collaborators),

---

[6] L. Pauling, "The Nature of the Chemical Bond," Cornell U. P., 1960.

ii) complete immiscibility, i.e., minimum number of Ge-Se (or Te) bonds,

iii) complete miscibility, with the number of Ge-Se (or Te) bonds a maximum at any composition.

From purely geometric arguments, it may be seen that the numbers of nearest neighbor bonds are as in Table 3 for Ge_xSe_{1-x} (or Ge_xTe_{1-x}). It can be noted that the sum of all nearest neighbor bonds is the same, regardless of model, provided the coordination at each atom is conserved.

In the case of Ge_xSe_{1-x} the atomic scattering factors vary very little for Ge-Ge, Ge-Se or Se-Se interferences, hence the area of the peaks in the rdf require negligible scattering factor correction. If it is assumed that the first peak in the rdf is due to overlapping Ge-Ge, Ge-Se and Se-Se contributions, then each model predicts the same area (or apparent average coordination number), 2(1+x), for the peak.

In the case of Ge_xTe_{1-x}, there is some variation in scattering factors and appreciable differences in the expected Ge-Ge, Ge-Te and Te-Te interatomic distances. If all of these interferences overlap to produce the first peak in the rdf then for each model we may plot both the expected uncorrected area of the first peak and also anticipate an expected change in peak shape as composition is varied.

Figure 6 shows a plot of calculated area under the first peak in the rdf before scattering factor correction for each of the three models considered. It can be seen

Table 3

Table showing the number and type of bonds contributing to the first peak and the anticipated area of the first peak for Ge_xSe_{1-x} and Ge_xTe_{1-x} according to three models:

1) random mixing of bonds
2) immiscibility, minimum number of bonds between unlike atoms
3) maximum number of bonds between unlike atoms.

			Maximum number of Ge-Se (or Te) bonds	
	Random bond mixing	Immiscible	$1 < x < 0.33$	$0.33 > x > 0$
p_{aa}	$2Nx^2$	$2Nx$	$N(3x-1)$	0
p_{bb}	$N(1-x)^2$	$N(1-x)$	0	$N(1-3x)$
p_{ab}	$3Nx(1-x)$	0	$2N(1-x)$	$4Nx$
Sum	$N(1+x)$	$N(1+x)$	$N(1+x)$	$N(1+x)$
Area of peak before correction	$4x^2f_1^2/F^2 + 2(1-x)^2f_1^2/F^2 + 6x(1-x)f_1f_2/F^2$	$4xf_1^2/F^2 + 2(1-x)f_1^2/F^2$	$2(3x-1)f_1^2/F^2 + 4(1-x)f_1f_2/F^2$	$2(1-3x)f_1^2/F^2 + 8xf_1f_2/F^2$

that the three curves lie close together, and could not be distinguished between by current rdf techniques, owing to experimental limitations. We may therefore conclude that the area of the first peak in the rdf is in this case a quantity peculiarly insensitive to the statistics of mixing. It should also be noted that the area under peaks obtained experimentally is determined with rather poor reliability, being sensitive to data inaccuracies, data treatment and value of glass density. (In contrast, peak locations are considerably more reliable.) Present work is directed to the breakdown of the rdf in more detail to try to establish a useful model of the atomic structure in these glasses.

Electron Microscopy

Figure 7a shows an electron micrograph from a glassy film of nominal composition $GeTe_2$. The conventional electron diffraction pattern is shown in 7b. It can be noted that only diffuse halos are present, indicating a glassy structure. The micrograph, however, does show some contrast on a scale of order 100 Å. The origin of this contrast has not been established, but is characteristic of all glassy materials including amorphous Ge and amorphous carbon films. Crystallites of 100 Å in size would give a sharp diffraction pattern. To understand the nature and origin of this structural inhomogeneity is of some importance in assessing the validity of contrasting electron transport theories

based on a homogeneous or alternatively heterogeneous structural model. For comparison, Fig. 7c shows a $GeTe_2$ film after recrystallization by beam heating inside the microscope. Large crystallites are now clearly visible and may be identified as a mixture of GeTe and Te from the diffraction pattern of Fig. 7d.

Kinetics of Crystallization

Films of Ge_xTe_{1-x} glasses were deposited to a thickness of 1 to 2 microns onto glass slides and on thin mica sheets. The slides were used for x-ray diffractometry studies and the mica sheets were employed in small angle x-ray scattering investigations.

The crystallization kinetics of these films was studied using a high angle x-ray diffractometer. Specimens were heat treated in air for various times at 200°C ± 5° and diffraction patterns were obtained by scanning over the 2θ angular range 20-60° using copper Kα radiation. Figures 8-10 show the intensity profiles versus time for some of the alloys examined. The change in breadth of the diffraction peak at half maximum intensity was plotted against the annealing time to obtain a measure of rate of crystallite growth as in Fig. 11. In addition, another measure of growth rate could be obtained by plotting peak height versus time at the annealing temperature as in Fig. 12. In the alloys studied so far the only crystallites to

appear consisted of elemental tellurium. It has been observed that the rate of appearance of crystalline Te is higher in the more Te-rich alloys. The rate is distinctly lower for the $GeTe_2$ film and the Te diffraction peaks have somewhat a different appearance in this case, the entire pattern never develops fully at the given heat treatments.

The growth of crystallites of Te unaccompanied by any other crystalline compound such as GeTe speaks against a massive crystallization of these films. The behavior is consistent with a local order model in which local $GeTe_4$ tetrahedra form, that is, the film in this model would show a tendency to separate into $GeTe_2$ and Te regions for the composition mentioned, and into Ge and $GeTe_2$ regions for compositions richer than Ge. On this model some phase separation is to be expected. Quite different annealing behavior is to be expected from compositions at either side of $GeTe_2$ in a composition diagram. This hypothesis is being tested and may be of some importance for mechanisms of memory switching. Studies of bond energies and Gibbs' free energy versus composition are being initiated to help provide a sound basis for the generation of structural models and to provide a key to the interpretation of kinetic crystallization data. Roy and collaborators[1] have noted already the strong tendency of the chalcogenide glasses to form immiscible glassy phase separated solutions. To examine this possibility further, small angle x-ray scattering measurements have been carried out on thick films on mica

using a Kratky small angle scattering camera. So far no change has been observed in the small angle scattering intensity with time of annealing; these experiments are to be repeated with higher sensitivity. Further techniques to examine possible phase separation are to be explored.

III. FAST NEUTRON AND γ-RAY EFFECTS IN AMORPHOUS SEMICONDUCTORS

Introduction

The unique range of properties exhibited by both insulating glass-ceramics and amorphous semiconductors makes them potentially useful in a variety of applications which may involve exposure to nuclear irradiation. Although the neutron radiation sensitivity of insulating glasses[7] and various crystalline ceramic materials[8-10] have been investigated in some detail, relatively little is known about neutron damage in semiconducting glasses.

Several recent reports have been made concerning neutron and γ-ray effects on the behavior of switching devices made of chalcogenide glasses,[11,12] The studies have shown

---

[7] E. Lell, N. J. Kreidl and J. R. Hensler, "Radiation Effects in Quartz, Silica and Glasses," Progress in Ceramic Science, Vol. 4, p. 73 (J. Burke, editor, Pergamon Press, 1966).

[8] W. Primak and R. Kampworth, "Radiation Compaction of Vitreous Silica," J. Appl. Phys., 39 [12] 5651-5658 (1968).

[9] M. Nachnam, L. Cojocaru and L. Ribco, Nukleonik, 10 Band, 1. Heft (1967), p. 1.

[10] Barber, "Effects of Nuclear Radiation on Electrical Properties of Non-stoichiometric NiO," J. Am. Cer. Soc., 51, 611 (1968).

[11] (a) S. R. Ovshinsky, E. J. Evans, D. L. Nelson, H. Fritzsche, "Radiation Hardness of Ovonic Devices," IEEE Trans. on Nuclear Science, Dec. 1968.
(b) R. R. Shanks, J. H. Helbers and D. L. Nelson, "Ovonic Computer Circuits Development," Technical Report AFAL-TR-69-309, June 1970.
(c) R. R. Shanks, D. L. Nelson, R. L. Rowler, H. C. Chambers and D. J. Neihaus, "Radiation Hardening Circuitry Using New Devices," Technical Report AFAL-TR-70-15, March 1970.

device insensitivity from fluences of 10^{16} n/cm^2 nvt fast neutron and 10^{11} rads/sec of γ-rays. The electrical conductivity of liquid chalcogenides has been found[13] to be unaffected by fast neutron dosages of as much as 1.8×10^{20} cm^{-2}. Considering that the measurements were made on liquids, this result is not surprising.

Results from this laboratory[14] have shown that the electrical conductivity of solid semiconducting glasses in the V_2O_5-P_2O_5 system are relatively unaffected by fast neutron fluences of up to 4×10^{17} nvt. However, an approximately 10% increase in electrical conductivity was observed after a dose of 1.25×10^8 rads of Co^{60} γ-ray irradiation. This behavior was attributed to an increase in the concentration of quasi-free charge carriers due to Compton scattering of electrons. Additional evidence in support of this argument will be presented here.

Studies of the influence of fast neutrons on the stability of the electrical properties of heterogeneous KPO_3-V_2O_5 semiconducting glasses have been recently reported by one of the authors.[15] An important observation in the study

---

[12] E. J. Evans, "A Feasibility Study of the Applications of Amorphous Semiconductors to Radiation Hardening of Electronic Devices," Picatinny Arsenal Technical Report 3698.

[13] J. T. Edmond, J. C. Male and P. F. Chester, J. Sci. Inst. (J. of Physics E), 1 [2] 373 (1968).

[14] L. L. Hench and G. A. Daughenbaugh, J. Nuclear Materials, 25, 58-63 (1968).

[15] L. L. Hench, J. Non-crystalline Solids, 2, 250-277 (1970).

was the degradation of electrical characteristics associated with 100 Å to 200 Å ordered heterogeneities within the glass matrix. After a 2.7×10^{17} nvt fluence the electrical conductivity had decreased by a factor of 7, A.C. conductivity characteristics of the disordered glass had appeared, and a large dielectric loss peak was destroyed. It is necessary, therefore, to discuss the importance of crystallite size on the fast neutron damage threshold in heterogeneous amorphous semiconductors.

Ionically conducting Li_2O-SiO_2 glasses containing submicron crystalline regions have also been shown by the authors to be strongly influenced by fast neutron exposure.[16] A fluence of 1×10^{17} nvt was sufficient to decrease the magnitude of the dielectric loss peak exhibited by the material. The radiation exposure also accelerated the sequence of crystallization reactions occurring during thermal treatment of the glass. The dissolution rate of lithium metasilicate crystals which appear as a precursor to equilibrium crystallization was enhanced by the fast neutron damage.

A final objective of this work is to compare the effects of the cumulative fast neutron dosage on the electrical properties of the nucleated Li_2O-SiO_2 glasses with the heterogeneous amorphous semiconductors studied in this program.

---

[16] W. D. Tuohig and L. L. Hench, J. Nuclear Materials, 31, 86-92 (1969).

Experimental Procedure

The glasses discussed were melted in electric muffle furnaces in covered Pt crucibles and formed into specimens approximately 1.8 cm in diameter and 0.5 cm thick by quenching into steel molds. The compositions studied, melting and annealing schedules are given in Table 4.

Table 4

Glass Composition	Melting Temp. and Time	Annealing Temp. and Time
80 mole % V_2O_5 - 20 mole % P_2O_5	966°C/10 hr.	300°C/30 min.
33 mole % KPO_3 - 67 mole % V_2O_5	550°C/8 hr.	200°C/2 hr.

Electrical measurements were made in vacuum on polished samples with vacuum evaporated gold electrodes in a double guard ring configuration using an apparatus previously described.[14,16,17]

Gamma-ray irradiation experiments were performed using a 30,000 Curie Co^{60} source at the University of Florida. The γ-ray dose was determined by using the photometric $Fe^{2+} \rightarrow Fe^{3+}$ reaction as detailed in ASTM procedure D-1671-63.[18]

---

[17] L. L. Hench, "Dielectric Relaxation in Materials Analysis," Society of Aerospace Materials and Process Engineers, Proceedings of the 14th Annual Symposium, Cocoa Beach, Florida, November 1968; reprinted as Technical Paper 428, Engineering Progress at the University of Florida, Gainesville.

[18] Test for absorbed gamma radiation dose in the Fricke Dosimeter, ASTM Standards, 29, 719 (1963).

Specimen temperature during γ-radiation was approximately 25°C.

The KPO_3-V_2O_5 glasses were given neutron irradiation exposures in the Wright-Patterson AFB reactor which has a fast neutron flux capability of 1.5×10^{13} n/cm^2 (>0.1 meV). The fast neutron flux was measured using a 58 nickel [n,p] 59 cobalt reaction with a 2.9 meV threshold energy. Fluxes reported are based on activations measured 48 hours after removal of the samples from the reactor. Cadmium wrapping was employed to protect the gold electrodes. Temperature monitoring of the reactor indicated that sample temperatures were in the range of 50°C throughout the exposures. Approximately four weeks lapse at 25°C between exposure and measurement was necessary to reduce activity to a tolerable level.

V_2O_5-P_2O_5 Amorphous Semiconductors

Previous reactor exposures of 80 mole % V_2O_5 - 20 mole % P_2O_5 glasses resulted in a slight increase in the electrical conductivity.[14] Separate Co^{60} γ-ray experiments indicated this behavior was due to γ-ray ionization of charge carriers. The net effect was only a 10% increase in conductivity. However, additional data presented in Fig. 13 shows that the γ-ray exposure strongly influences the dielectric losses in the glasses.

The dielectric loss angle, tan δ, plotted as a function of log measuring frequency, Hz, increases due to the

6.8×10^7 rads γ-ray exposure. Well resolved dielectric loss peaks also appear. The frequency location of the loss peaks and their magnitude both suggest that appreciable interfacial polarization is occurring in the irradiated glasses.[19] Analysis of the temperature dependence of the frequency location of the dielectric loss peak,

$$f_{max} = f_o \exp[-Q/RT], \qquad (1)$$

results in a measured activation energy for the loss process of 0.6 ev. This is the same value calculated for the temperature dependence of the D.C. conductivity of this glass.[15] Therefore, it is reasonable to assume that similar electronic carriers are involved in the relaxation process as contribute to the D.C. conductivity.

Since the γ-irradiation should not produce structural heterogeneities in the glass, the interfacial barriers involved in the relaxation process must be associated with heterogeneities already present or the sample electrodes. As discussed in a recent paper concerning the theory of heterogeneous semiconductors,[20] either internal heterogeneities or partially blocking electrodes can give rise to dielectric loss peaks in these materials.

---

[19] L. K. H. von Beek, in Progress in Dielectrics, Vol. 7 (CRC Press), p. 69.

[20] L. L. Hench and H. F. Schaake, "Electrical Properties of Glass," in Introduction to Glass Science, D. Pye and H. Simpson, editors, Plenum Press (in Press).

A γ-ray dosage of 1.25×10^8 rads produced an unusual low frequency resonance-like response which also appears to be an interfacial phenomena. Figure 14 summarizes a series of measurements of the frequency dependent capacitance of the 80/20 V_2O_5-P_2O_5 glass exposed to 1.25×10^8 rads. After irradiation an appreciable increase in the capacitance is observed even at 23°C. At 40°C, post radiation, a large increase in capacitance occurs, followed at 65°C by a wide low frequency resonance-like effect. The capacitance of the sample is negative over the range from 2.7×10^3 Hz to 4.5×10^5 Hz, as measured by the -C scale on the Wayne Kerr B-221 bridge and the L scale on the B-601 bridge. From 3×10^4 Hz to 1×10^5 Hz the negative C values are too large to be measured.

At a higher temperature, 87°C, the resonance-like behavior appears to be damped and is measurable over the entire frequency range. At 114°C the negative capacitance behavior disappeared during the measurements, indicating a rapid annealing process at this temperature. Post annealing data is shown in Fig. 14 at a measurement temperature of 86°C. After annealing, capacitance values are nearly equivalent to the pre-radiation values for the glass and are not shown for the sake of clarity.

It seems that the data of Figs. 13 and 14 can be interpreted in one of two ways. Either the ionizing radiation produces extra charge carriers which are trapped at previously existing barriers in the glass or at the electrode-

glass interface. Or, the radiation could create traps at interfacial regions which are populated with "normal" carriers, the traps being created by ionization of deep-lying electrons. The fact that the activation energy for the relaxation loss process is the same as for D.C. conduction would appear to favor the latter alternative. One would expect a lower activation energy for a large number of ionized electrons. Also, if pre-existing traps at interfaces were present, the relaxation process should occur with "normal" carriers as well.

Creation of a wide distribution of deep-lying traps at interfacial regions also provides a reasonable explanation for the observed resonance behavior at 1.25×10^8 rads. In such a model, the resonance-like behavior is associated with thermally activated and field directed oscillations between trapping sites. At low temperatures, the oscillations simply contribute an additional interfacial polarization to the capacitance. At sufficiently high temperatures, resonance oscillations through the barriers become possible. A portion of the population obtains irreversible sites on one side of the barrier, thus producing a temperature dependent annealing of the phenomena.

Partially Crystallized Semiconducting Glasses

Previously reported investigations of fast neutron effects in heterogeneous 33 mole % KPO_3 - 67 mole % V_2O_5 semiconducting glasses involved crystallites in the 100-200 Å

size range.[10,21] A heat treatment at 288°C of glasses rapidly quenched from 800°C was employed in the nucleation and growth of the crystallites. The studies showed that fast neutron fluences of less than 1.0×10^{17} were required to destroy dielectric loss peaks associated with the high conductivity crystallites.

It is also possible to produce a small volume fraction, <1%, of sub-micron crystals in the KPO_3-V_2O_5 glasses by casting from temperatures of 550°C or below.[15] Dielectric loss peaks are exhibited by such materials as shown in Fig. 15. The loss peaks have been attributed to high conductivity PV_2 crystals, giving rise to Maxwell-Wagner-Sillars (MWS) interfacial polarization.[22] Similar behavior has been observed in the FeO-P_2O_5 system.[23] The size of the crystals in the sample of Fig. 15 are in the range of 0.1μm, a factor of 10 larger than in the previously reported study.[15]

The effect of the exposure of the heterogeneous glass to a 1.7×10^{17} nvt fast neutrons is also shown in Fig. 15. Two major changes are readily apparent. The magnitude of the loss peak is markedly reduced and the location of the

---

[21] L. L. Hench, A. E. Clark and D. L. Kinser, "Neutron Irradiation Effects in Partially Crystallized Semiconducting Glasses," submitted to J. Non-crystalline Sol.

[22] A. Fuwa, "Electrical Properties of Glasses and Crystals in the K_2O-V_2O_5-P_2O_5 System," M.S. Thesis, University of Florida, 1970.

[23] D. L. Kinser, J. Electrochem. Soc., 117 [4] 546 (1970).

loss peak is shifted to a higher frequency. In terms of the MWS interfacial polarization model, the decrease in loss peak height indicates that either the volume fraction of crystallites has decreased or the conductivity difference between the phases is reduced, or the phase boundary has been degraded sufficiently that it will not sustain a space charge.

The frequency location of the loss peak is controlled by the morphology of the dispersed phase and consequently, a shift in frequency is evidence that morphological changes have occurred. Consequently, the loss behavior observed indicates that there is cumulative disordering of the dispersed sub-micron crystals within the glass matrix from the fast neutron irradiation. The damage threshold for the larger crystals appears to be in the range of an order of magnitude greater than the 100-200 Å crystals. Consequently, these results would suggest that the damage threshold for crystals dispersed in a glass matrix may be linearly proportional to the size of the crystals. Additional studies to extend the range of validity of this conclusion are in progress.

Previous investigations have established that heat treating 33 mole % Li_2O-SiO_2 glasses at 500°C for 5-6 hours precipitates metastable lithium metasilicate crystals that are ~200 Å long and 50 Å wide.[24,25] A MWS dielectric loss

---

[24] D. L. Kinser and L. L. Hench, J. Am. Cer. Soc., 52, 445 (1968).

[25] D. L. Kinser and L. L. Hench, J. Materials Sci., 5, 369 (1970).

peak appears in the glass concurrent with the presence of the crystals. Additional heat treatment causes the metastable crystals to resorb and nucleate the equilibrium lithium disilicate crystal phase in the process. The dielectric loss peak decreases in magnitude and shifts to a higher frequency as a result of the resorbtion.

A recent paper by the authors showed that the metastable nucleation process was unaltered by a 1.0×10^{17} nvt irradiation of the glass prior to heat treatment.[16] However, the metasilicate dissolution process was shown to be significantly accelerated by the fast neutron irradiation. The explanation proposed was that the Li^+ mobility was enhanced by the irradiation, making the structure more susceptible to thermal alteration. An enhanced mobility of the Li ions would also decrease the conductivity difference between the matrix and the crystals, thereby reducing the magnitude of the loss peak, as recently shown.[26] The absence of a shift in frequency of the peak with the 1.0×10^{17} nvt exposure indicates that appreciable morphological changes did not occur.

Recent results have shown that increasing the fast neutron fluence to 1.8×10^{17} continues the degradation of the dielectric loss peak in the heterogeneous Li_2O-$2SiO_2$ glasses

---

[26] L. L. Hench, W. D. Tuohig and A. E. Clark, "Fast Neutron Effects in Glass-Ceramics and Amorphous Semiconductors," to be published in proceedings of Ceramics in Severe Environments Conference, North Carolina State University, December 1970, Plenum Press, publisher, H. Palmour and W. Kreigel, editors.

to one-third the magnitude of the pre-radiation peak.[20] In addition, the location of the peak is shifted to higher frequencies. This result is analogous to the loss peak changes observed for the irradiation of the heterogeneous amorphous semiconductors studied. The damage threshold for the KPO_3-V_2O_5 system appears to be lower, however, as a result of lower bond energies in the glass structure. Thus, it appears that the structurally dependent radiation damage in heterogeneous amorphous semiconductors is a result of enhanced ionic mobility at low dosages (1.0×10^{17} or less) followed by neutron destruction of the sub-micron crystal nuclei at larger dosages.

Conclusions

The major point to be re-emphasized is that the electrical properties of heterogeneous glasses that are governed by sub-micron crystals are susceptible to fast neutron damage at fluences of $1\text{-}2 \times 10^{17}$ nvt. The size of the crystals affects the damage threshold. Ionizing radiation produces electronic complications in addition to the neutron related structural changes for semiconducting glasses.

FIGURE CAPTIONS

Figure 1. a) Intensity of elastically scattered electrons vs. $2\sin\theta/\lambda$ for a GeSe film

b) experimental pair distribution curve

c) experimental radial distribution function.

Figure 2. a) Intensity of elastically scattered electrons vs. $2\sin\theta/\lambda$ for a $GeSe_2$ film

b) experimental pair distribution curve

c) experimental radial distribution function.

Figure 3. a) Intensity of elastically scattered electrons vs. $2\sin\theta/\lambda$ for several films of nominal composition $GeTe_2$. It is not known whether the variation between the curves is due to compositional variations or to differences in order.

b) The pair distribution curves from the data of (a)

c) radial distribution functions. Note the shift in zero base line between the curves.

Figure 4. a) Intensity of elastically scattered electrons vs. $2\sin\theta/\lambda$ for two films of $GeTe_4$

b) the resulting pair distribution functions

c) radial distribution functions.

Figure 5. a) Plot of ionic radii of Ge, Se and Te versus ionic charge. Ge is referred to the lower scale, Se and Te are referred to the upper scale.

b) Sum of the ionic radii for Ge-Se and Ge-Te nearest neighbors.

Figure 6. Plot of expected experimental area under the first peak in the rdf of Ge_xTe_{1-x} according to three models:

a) random mixing of bonds

b) immiscible, minimum number of Ge-Te bonds

c) maximum number of Ge-Te bonds at all times

d) all of the models lie on the dotted line in the case of Ge_xSe_{1-x}.

Figure 7. a) Electron micrograph of glassy $GeTe_2$ film at 92,600X. A fine contrast pattern is visible.

b) The diffuse diffraction pattern of (a) showing glassy condition of film.

c) After crystallization inside the microscope, large crystallites are visible. Magnifications as in (a).

d) Electron diffraction pattern now has sharp rings and indicates the presence of crystalline GeTe and Te.

Figure 8. Intensity versus 2θ for films of $GeTe_2$. The curves correspond to annealing times of 1, 8, 16, 32 and 64 minutes at 200°C.

Figure 9. Intensity versus 2θ for $GeTe_{5.5}$. The initial curve is of the glassy film before heat treatment. The second curve is after 7 minutes at 200°C.

Figure 10. Intensity versus 2θ for $Ge_3Te_{16}As$. The peaks grow in intensity with heat treatment. The curves correspond to 0, 2 and 6 minutes at 200°C.

Figure 11. Peak breadth at half height versus total time at 200°C for the five compositions examined.

Figure 12. Peak height with background subtracted versus total time at 200°C for the five compositions examined.

Figure 13. Development of dielectric loss peaks in an 80 mole % V_2O_5 - 20 mole % P_2O_5 semiconducting glass with a 6.8×10^7 rads ^{60}Co γ-ray exposure.

Figure 14. Sequence of capacitance behavior of our 80/20 V_2O_5/P_2O_5 semiconducting glass after 1.2×10^8 rads ^{60}Co γ-ray irradiation. Sequence: 23°C pre-rad; 23°C post-rad; 65°C post-rad; 87°C post-rad, 86°C post-rad, post 119°C annealing; 41°C post-rad, post annealing.

Figure 15. Dielectric loss peaks, before and after 1.7×10^{17} nvt irradiation, exhibited by a 33 mole % KPO_3 - 67 mole % V_2O_5 semiconducting glass-ceramic.

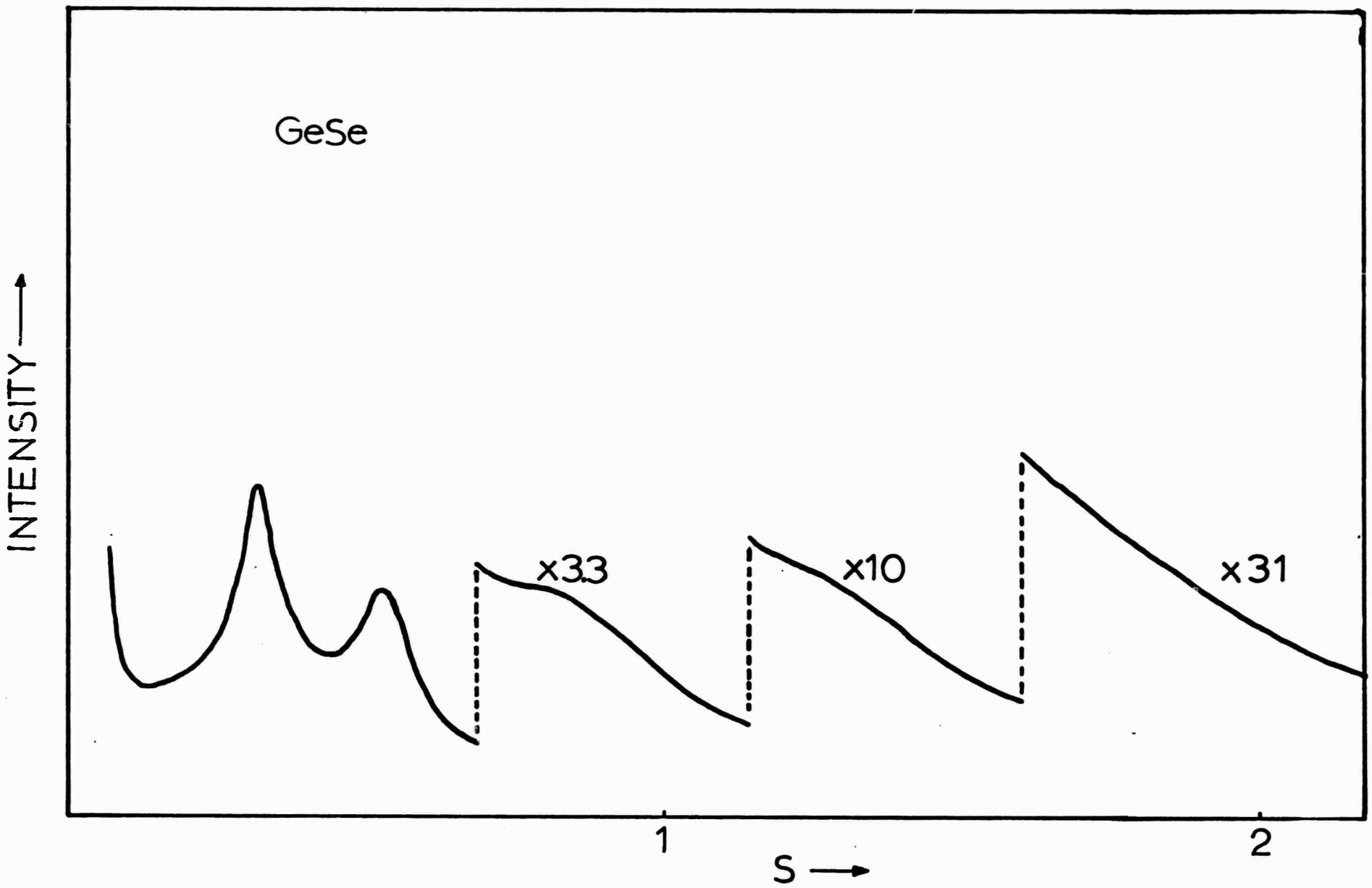

Figure 1a.

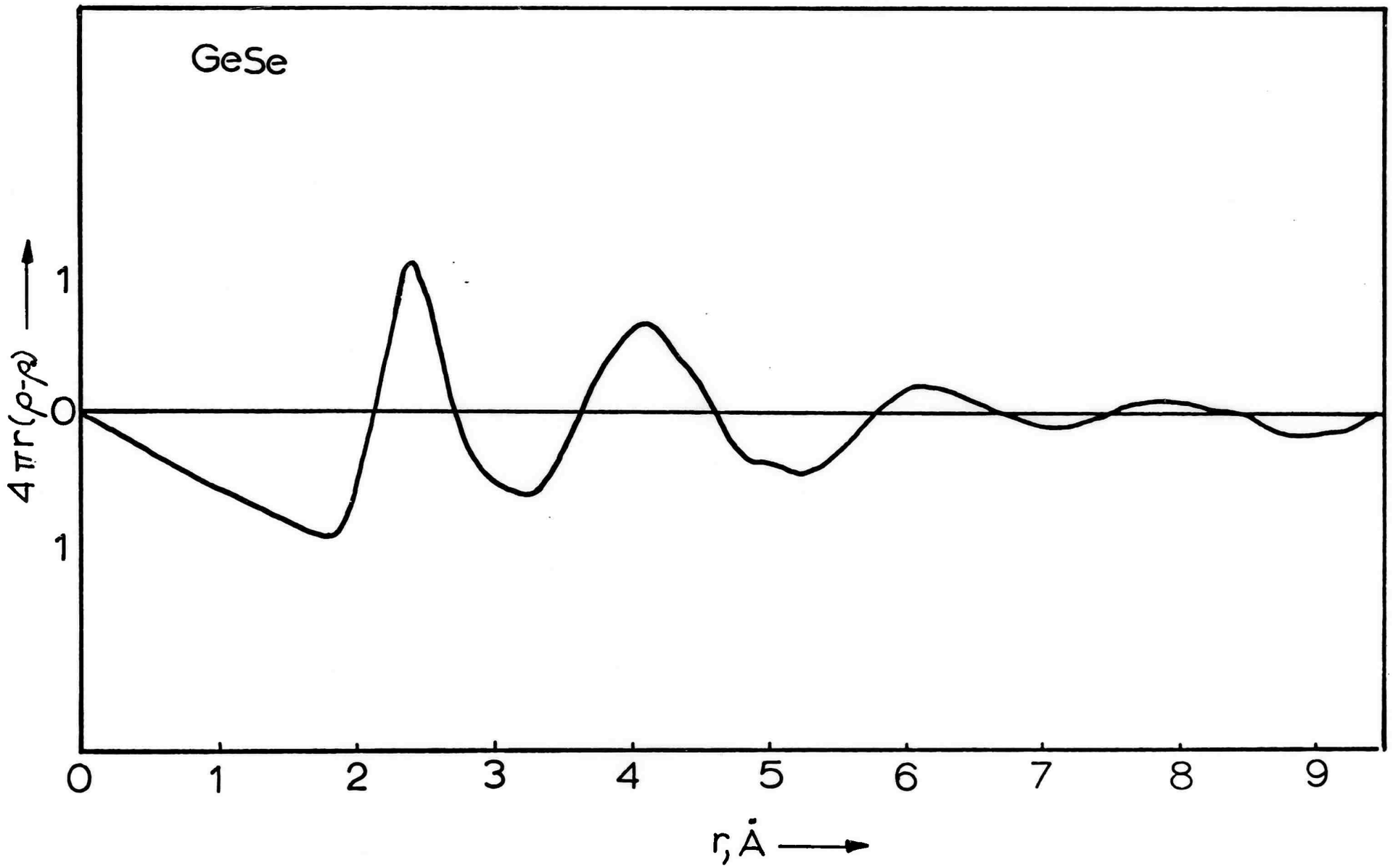

Figure 1b.

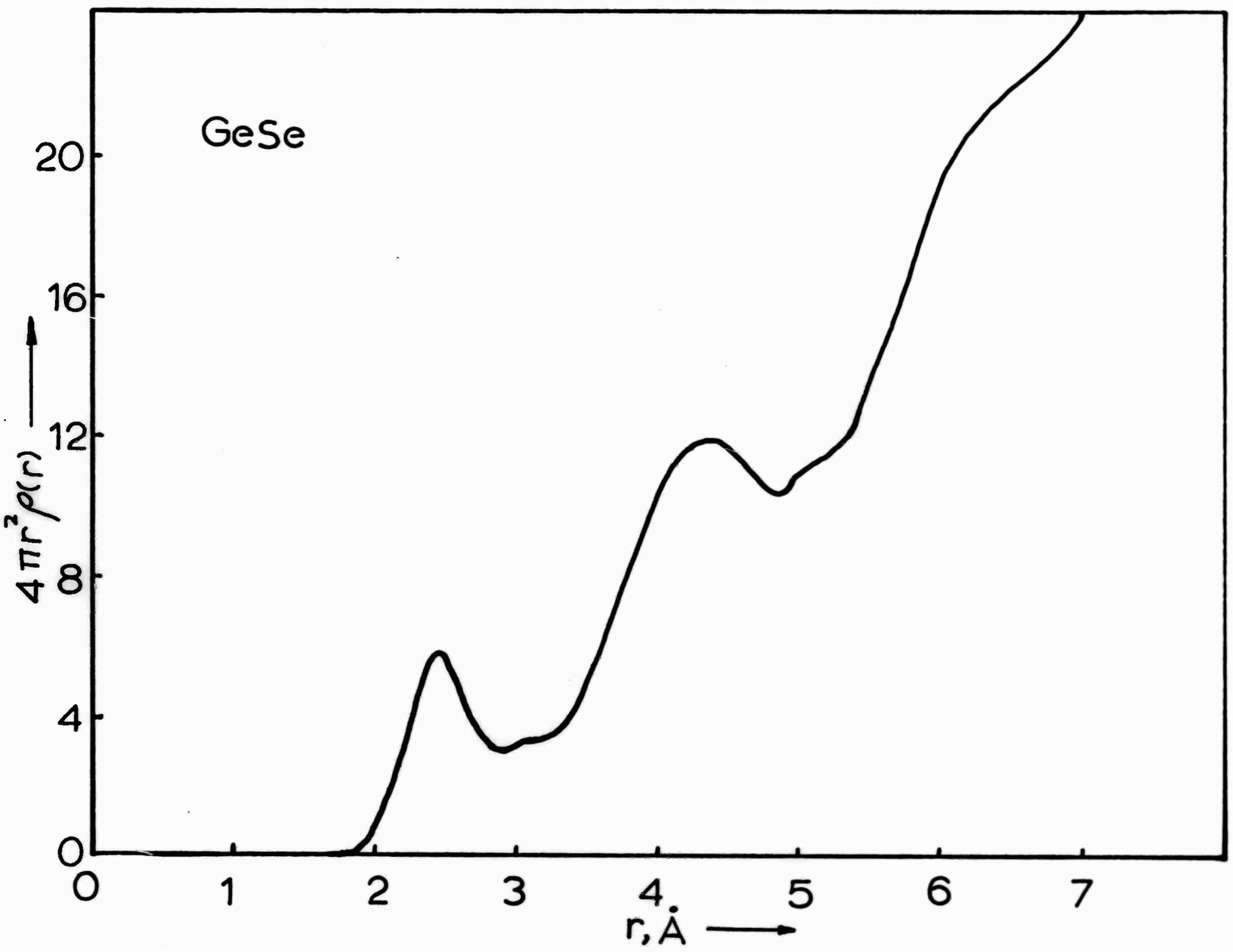

Figure 1c.

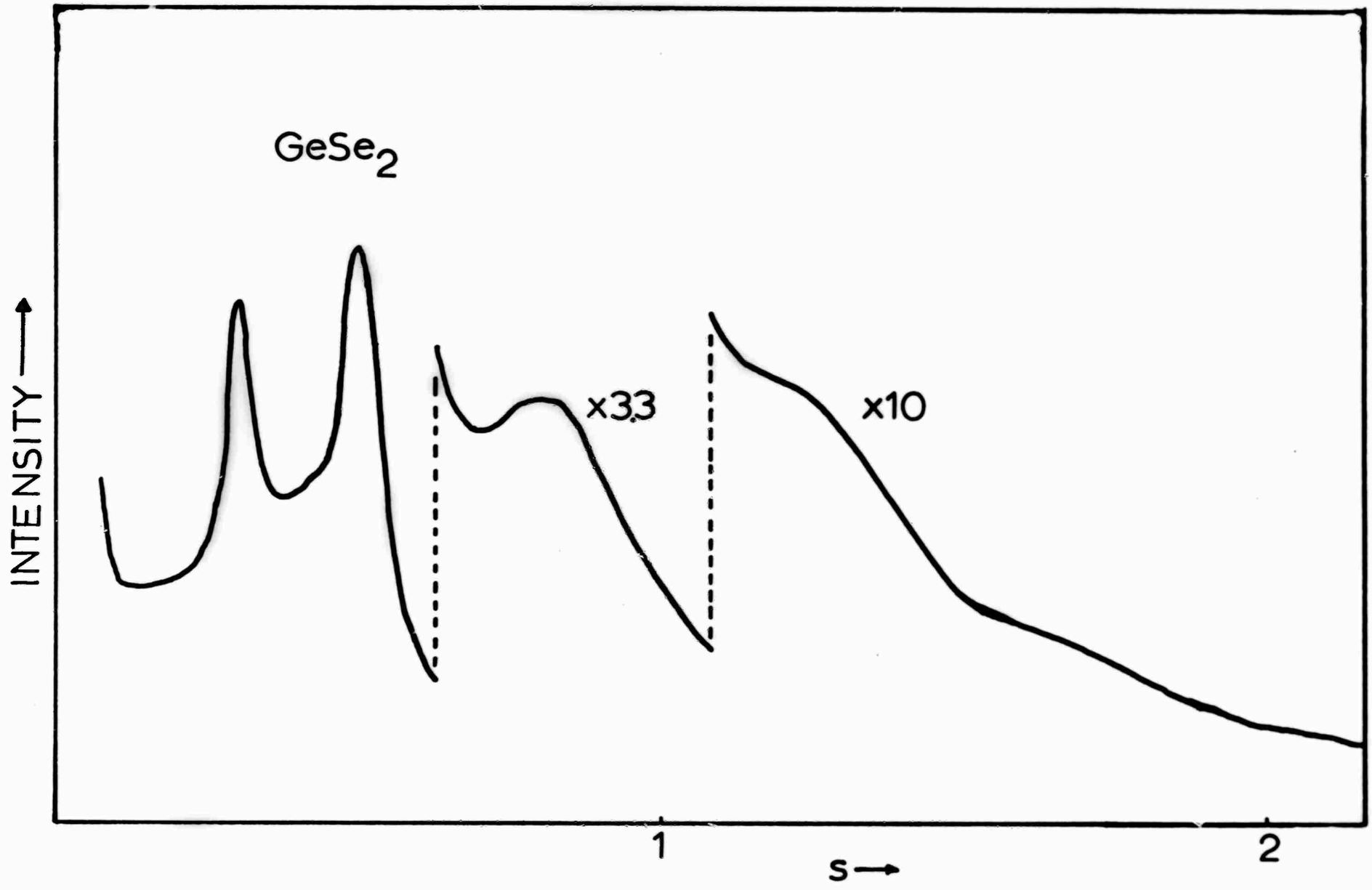

Figure 2a.

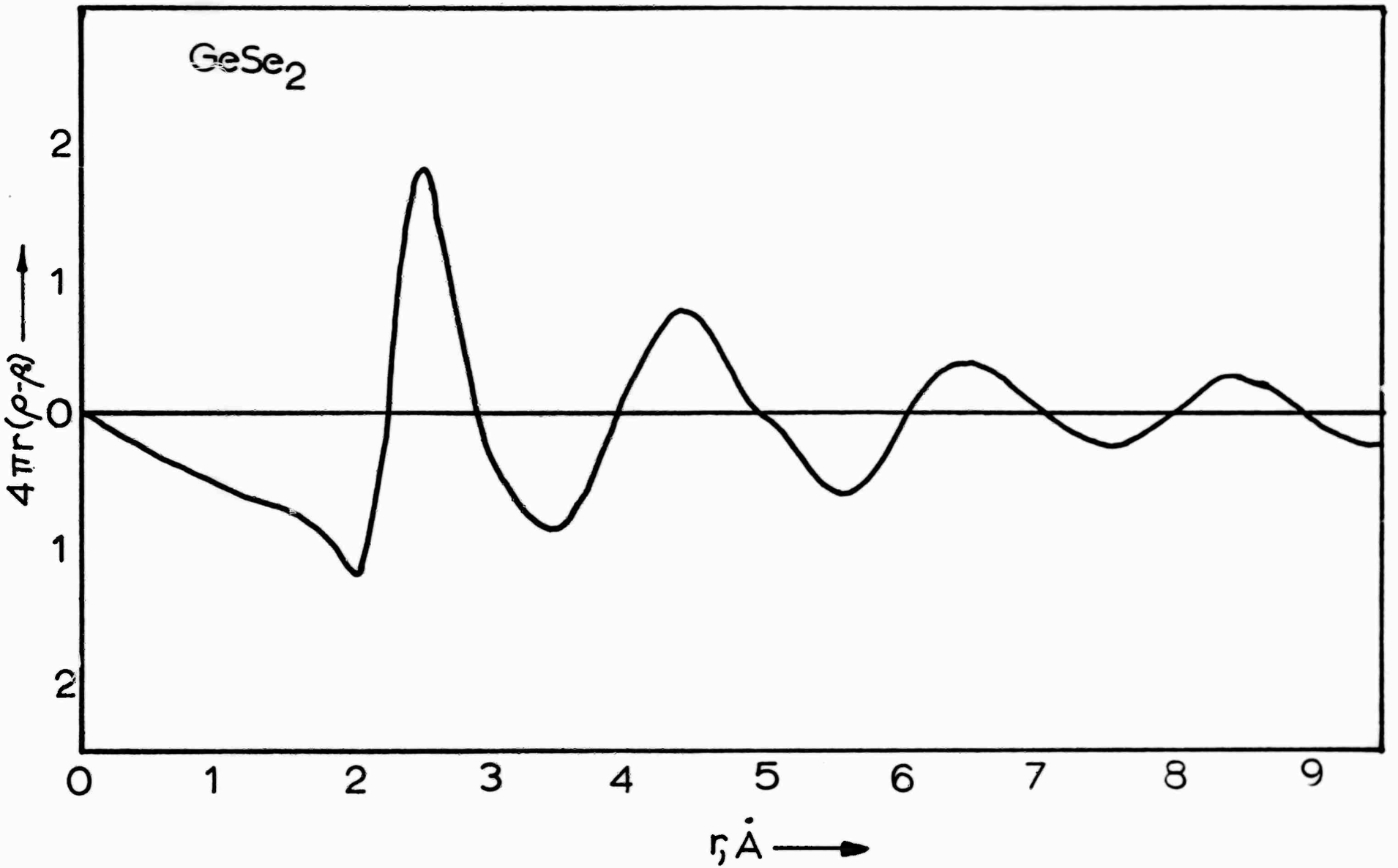

Figure 2b.

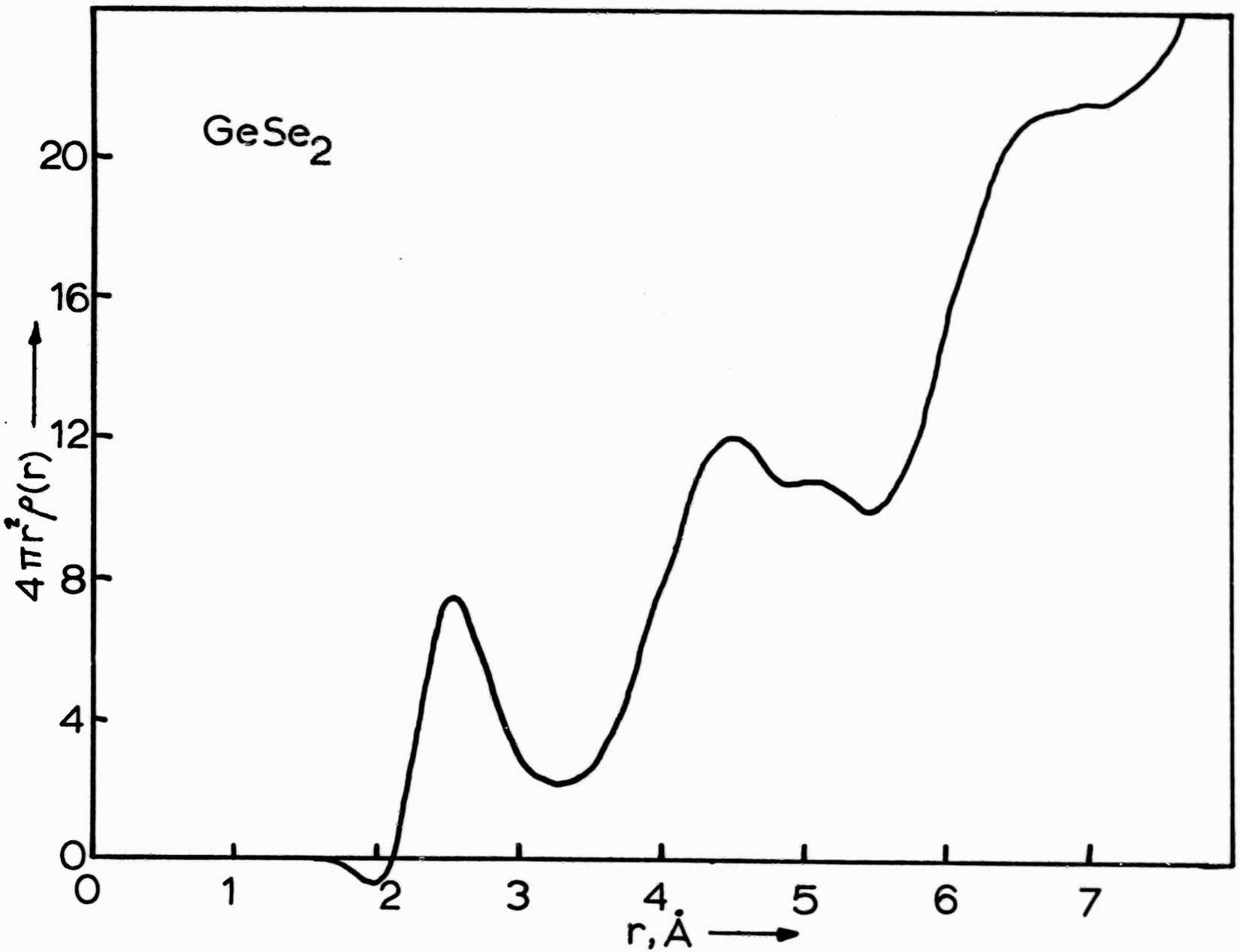

Figure 2c.

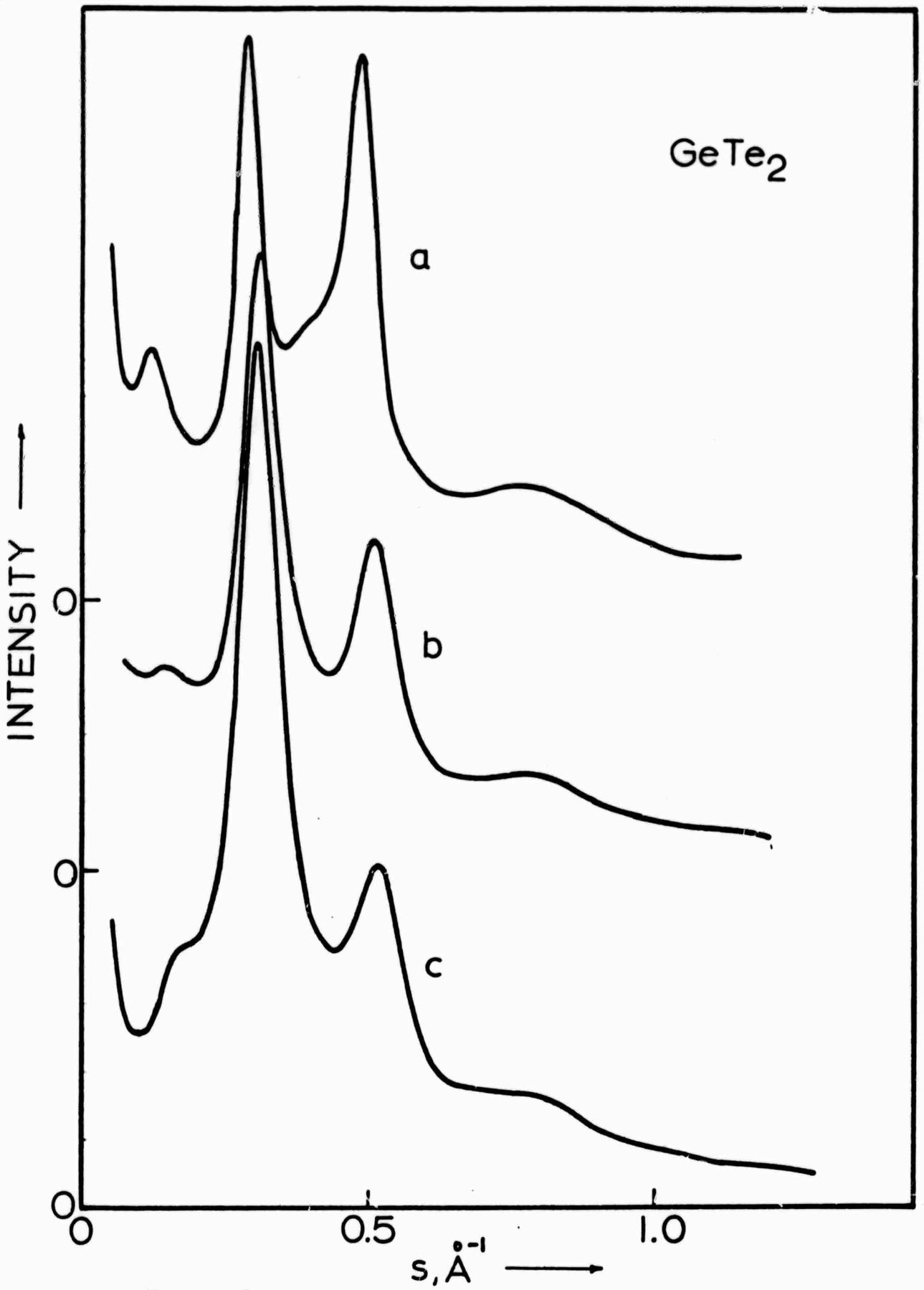

Figure 3a.

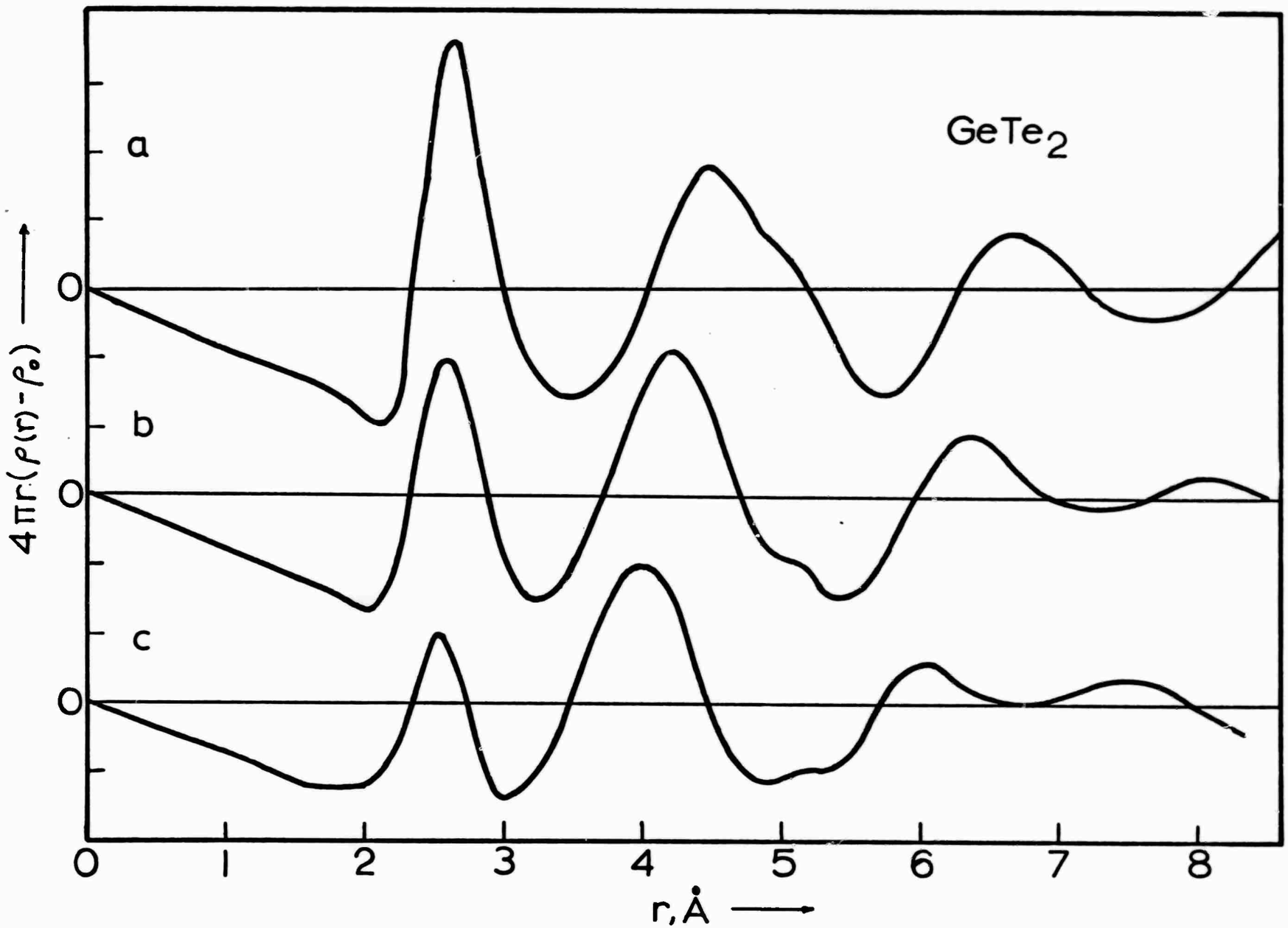

Figure 3b.

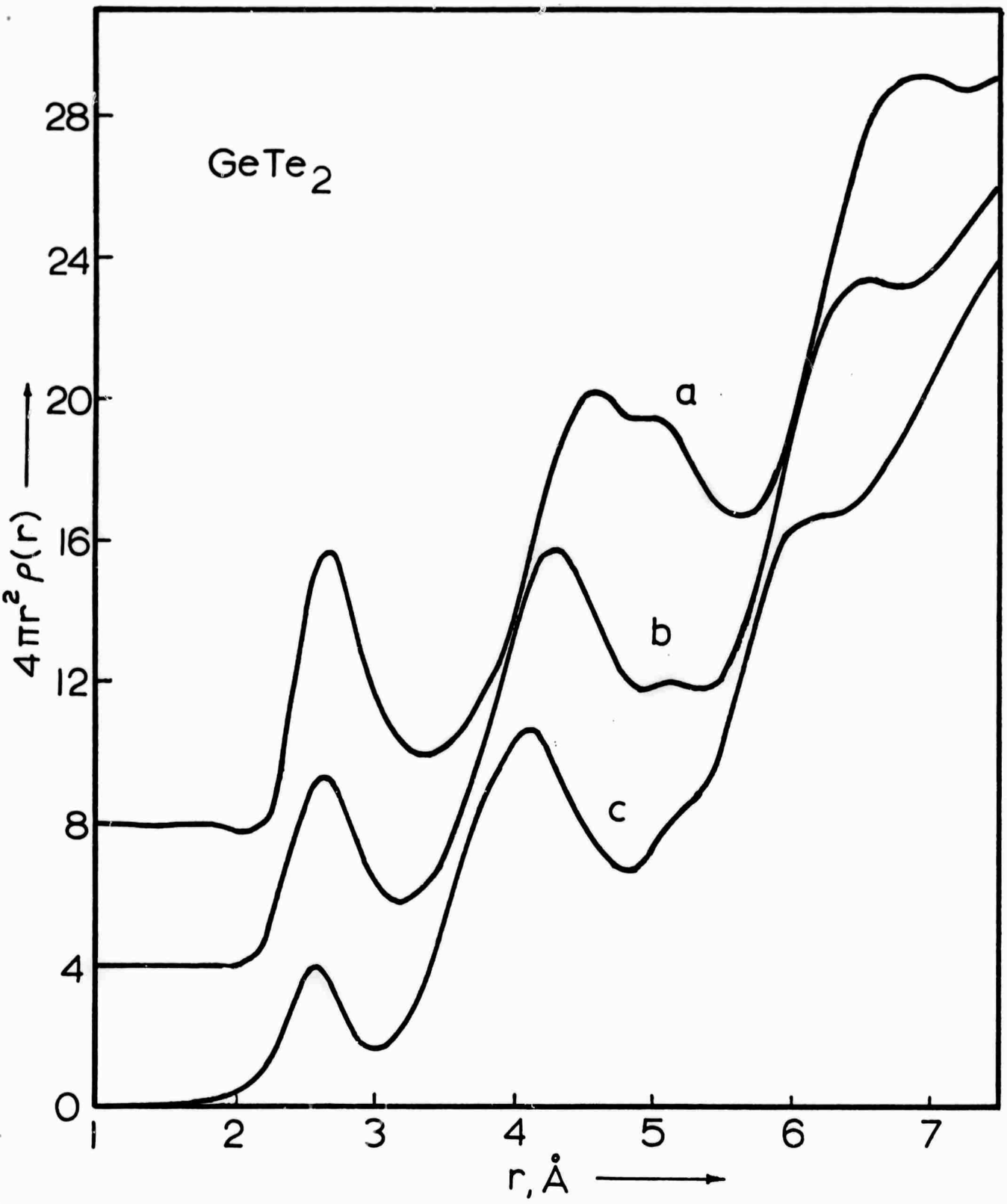

Figure 3c.

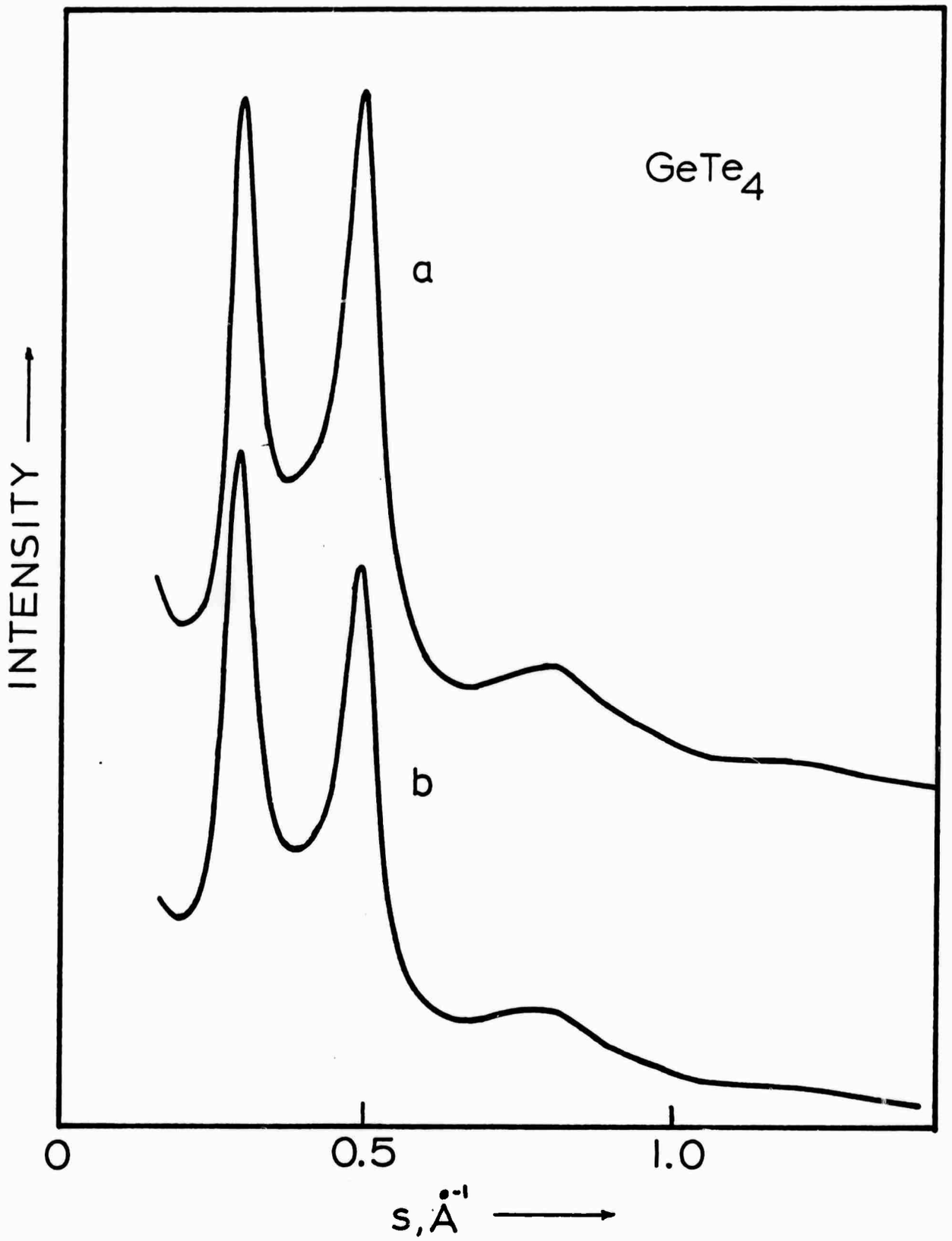

Figure 4a.

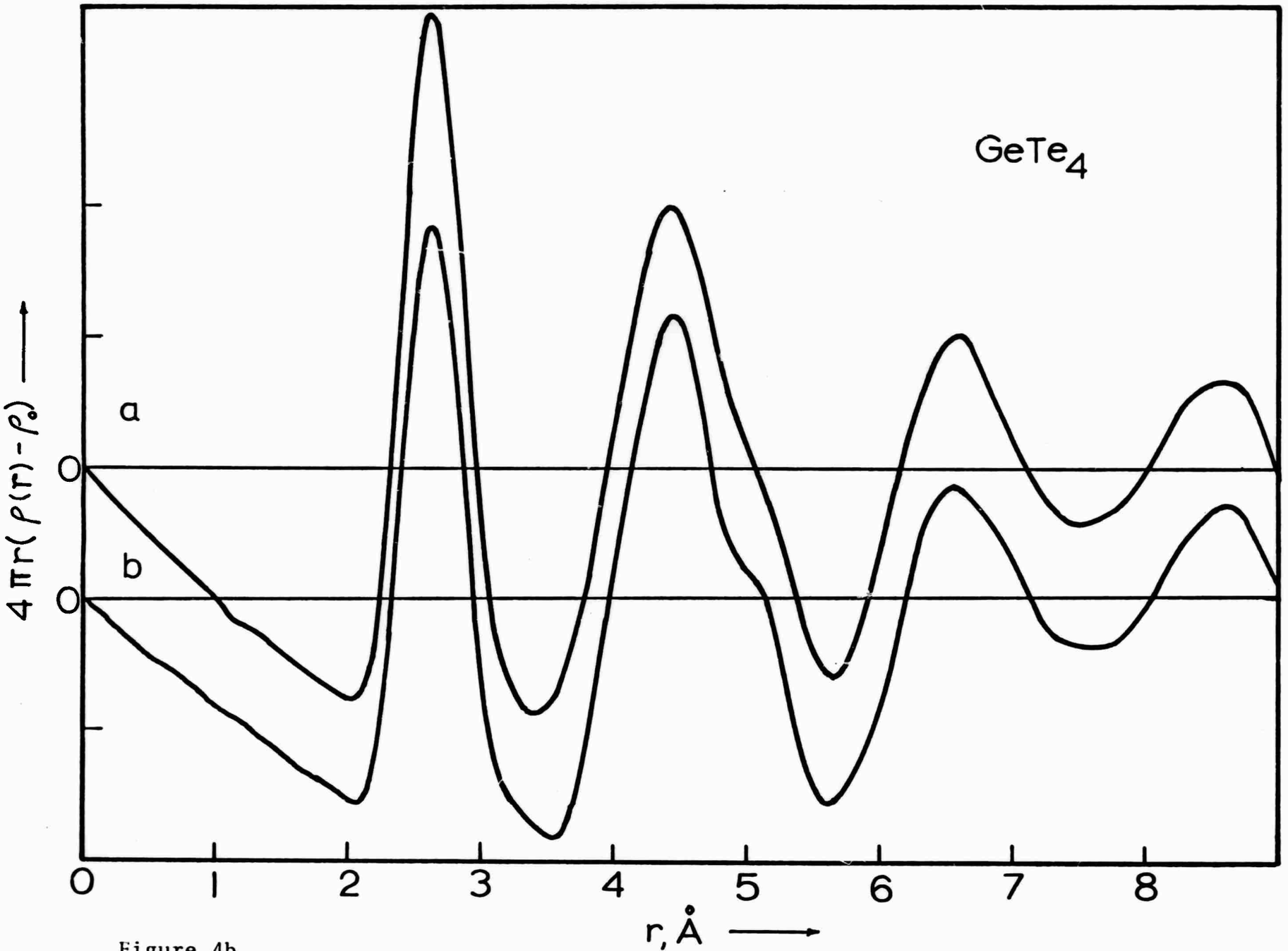

Figure 4b.

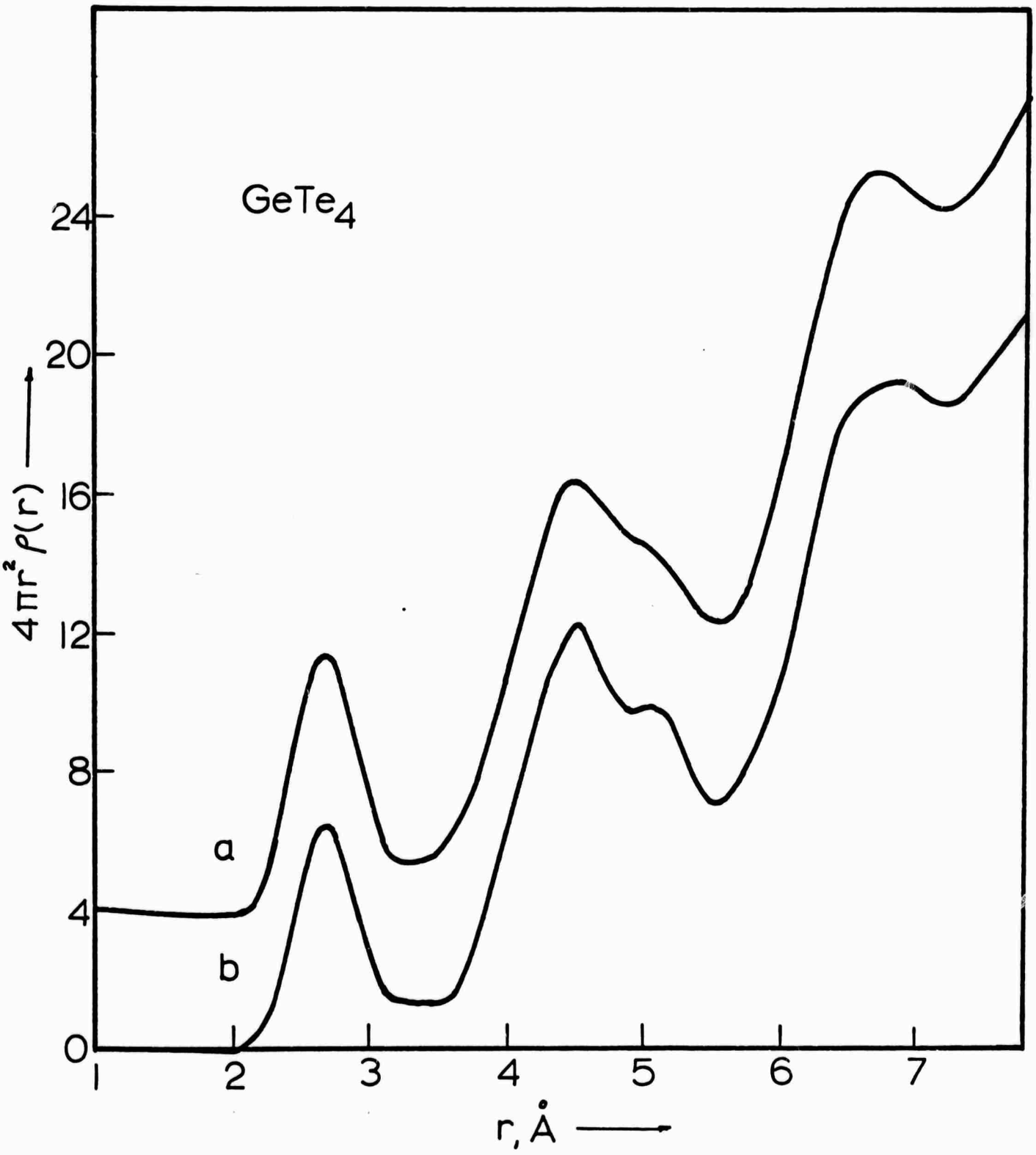

Figure 4c.

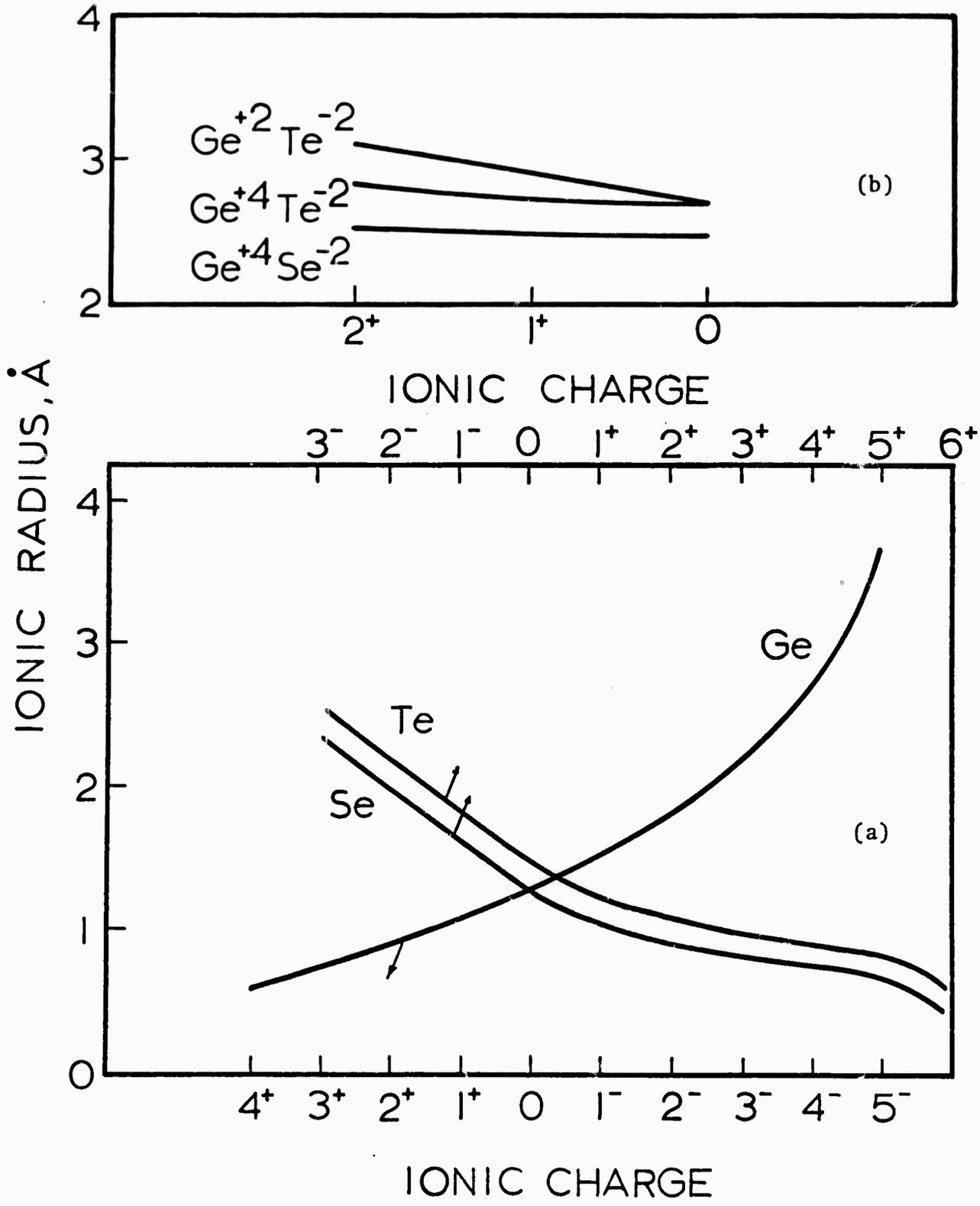
4
3
2
$Ge^{+2}Te^{-2}$
$Ge^{+4}Te^{-2}$
$Ge^{+4}Se^{-2}$
(b)
2+
1+
0
IONIC CHARGE
3- 2- 1- 0 1+ 2+ 3+ 4+ 5+ 6+
IONIC RADIUS, Å
4
3
2
1
0
Ge
Te
Se
(a)
4+ 3+ 2+ 1+ 0 1- 2- 3- 4- 5-
IONIC CHARGE

Figure 5.

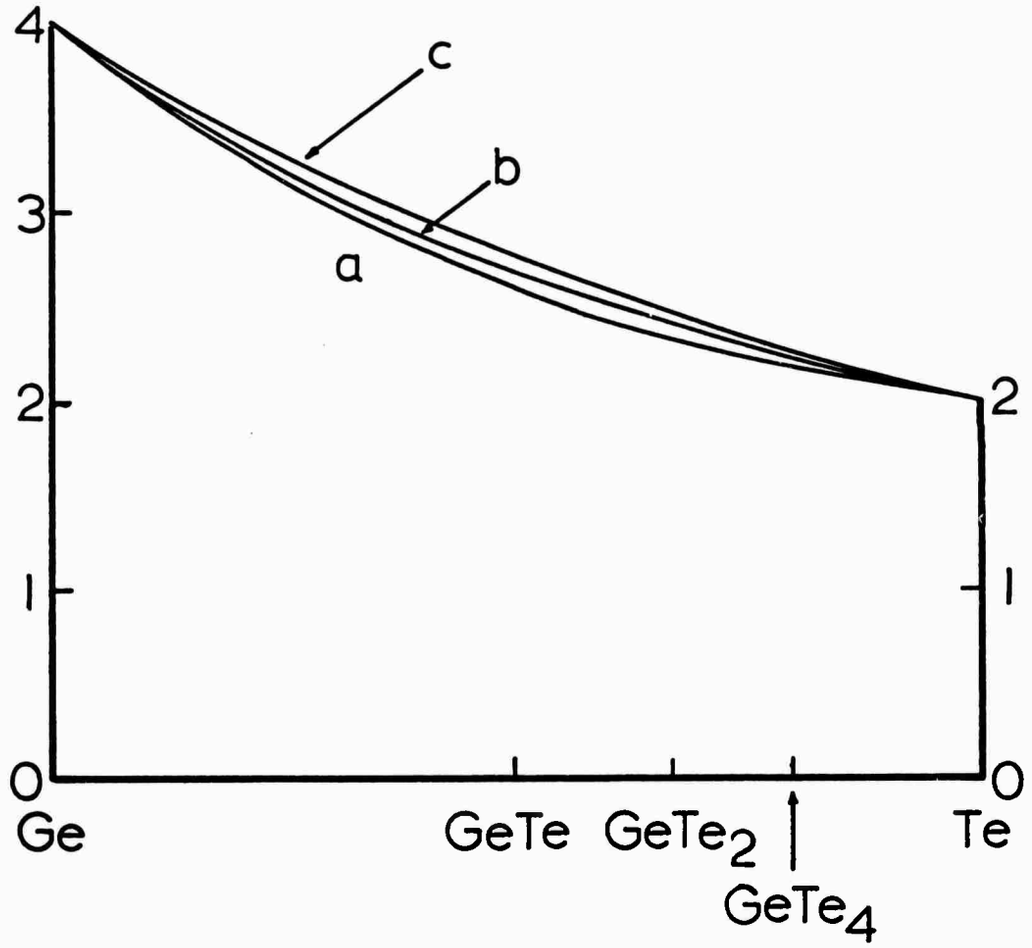

Figure 6.

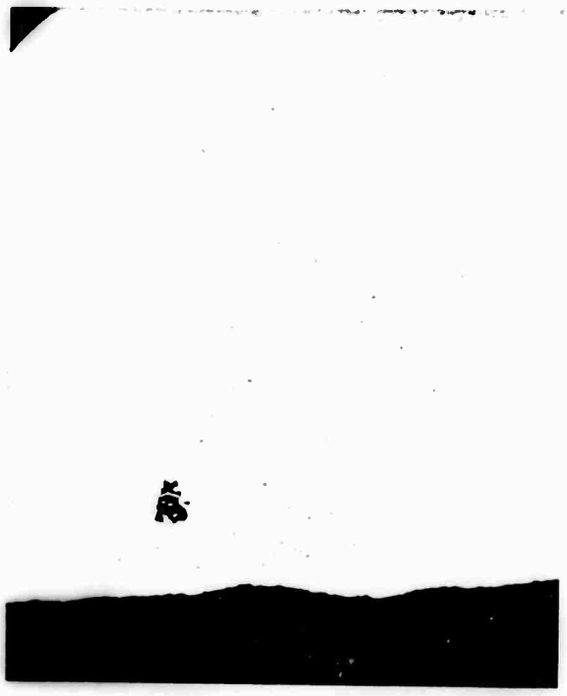

(a)

(c)

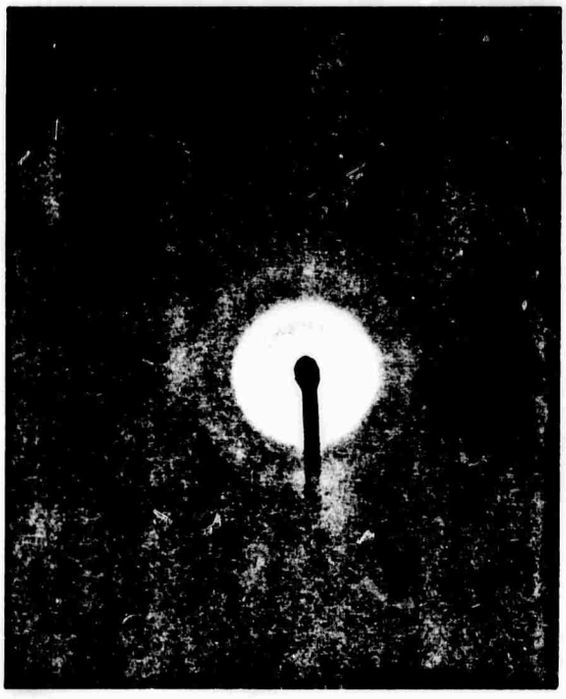

(b)

(d)

Figure 7.

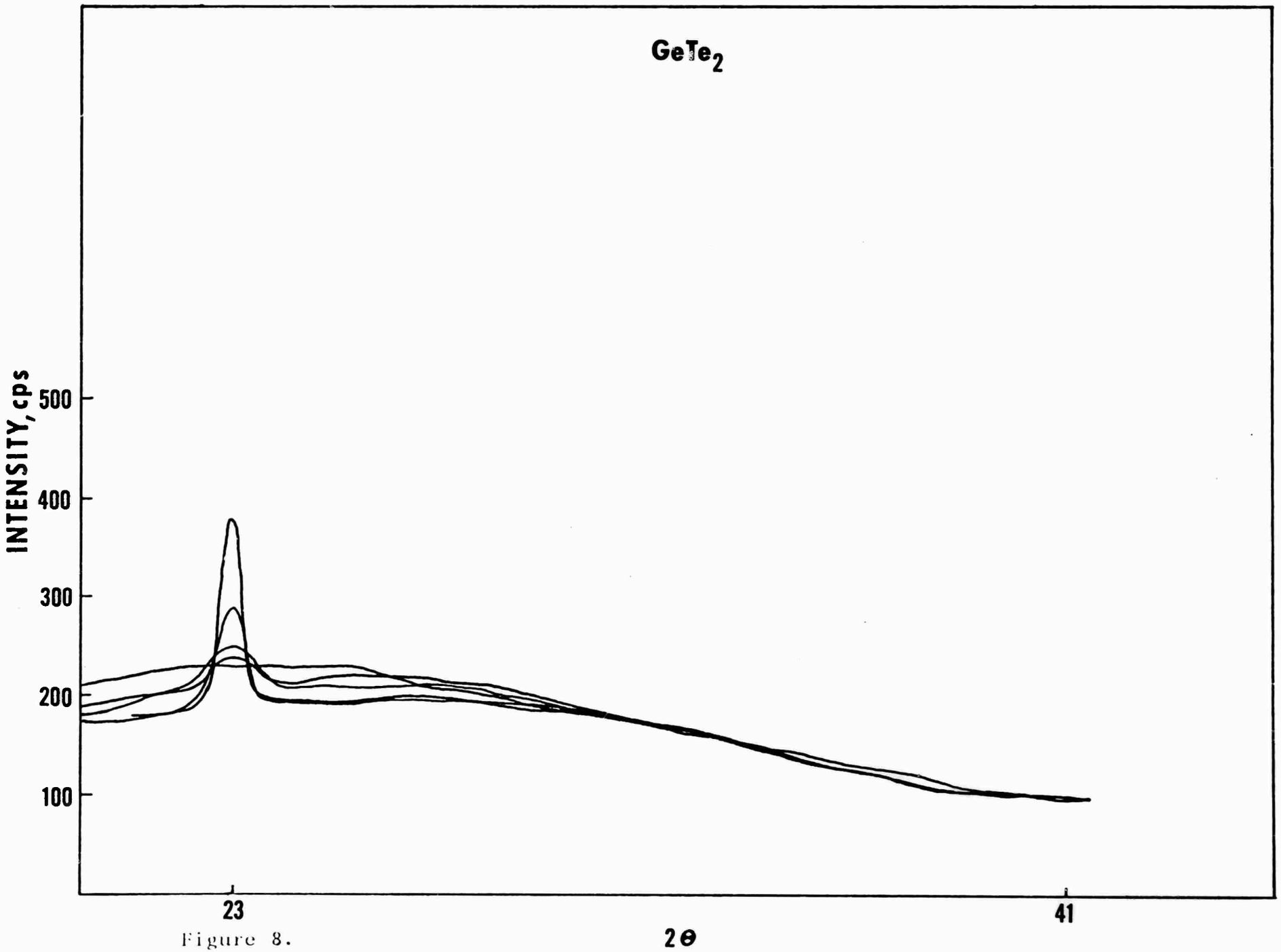

Figure 8.

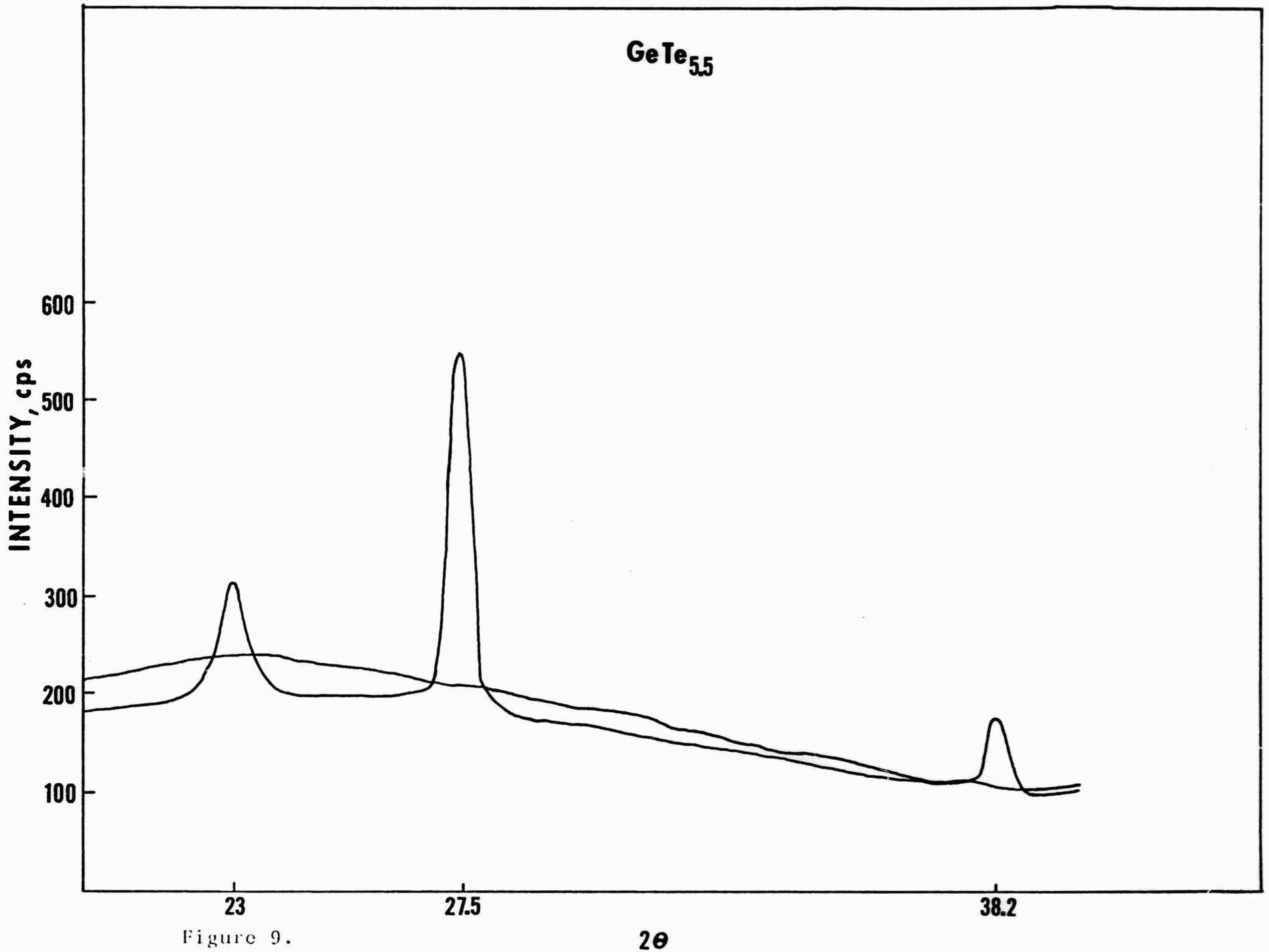

Figure 9.

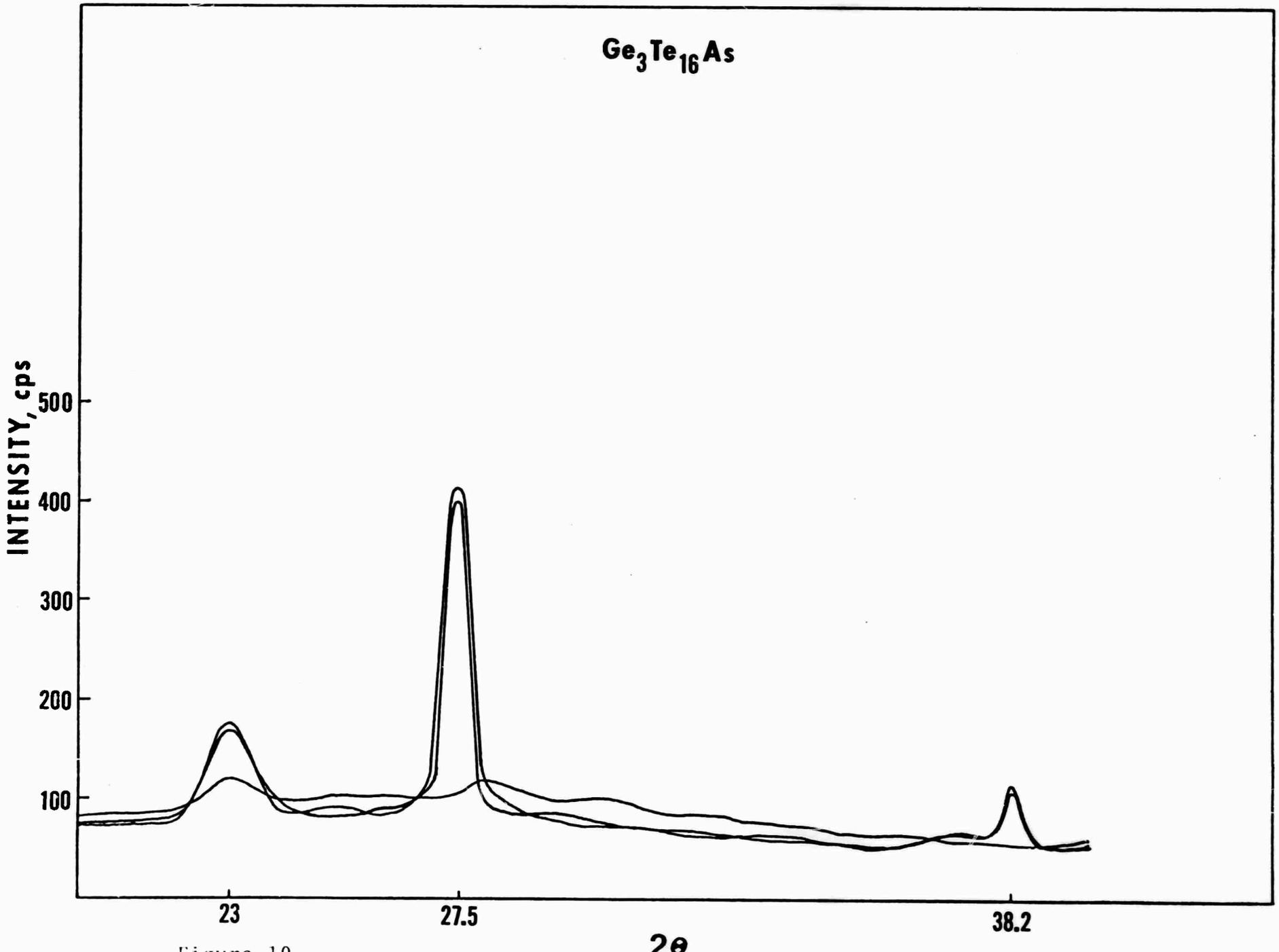

Figure 10.

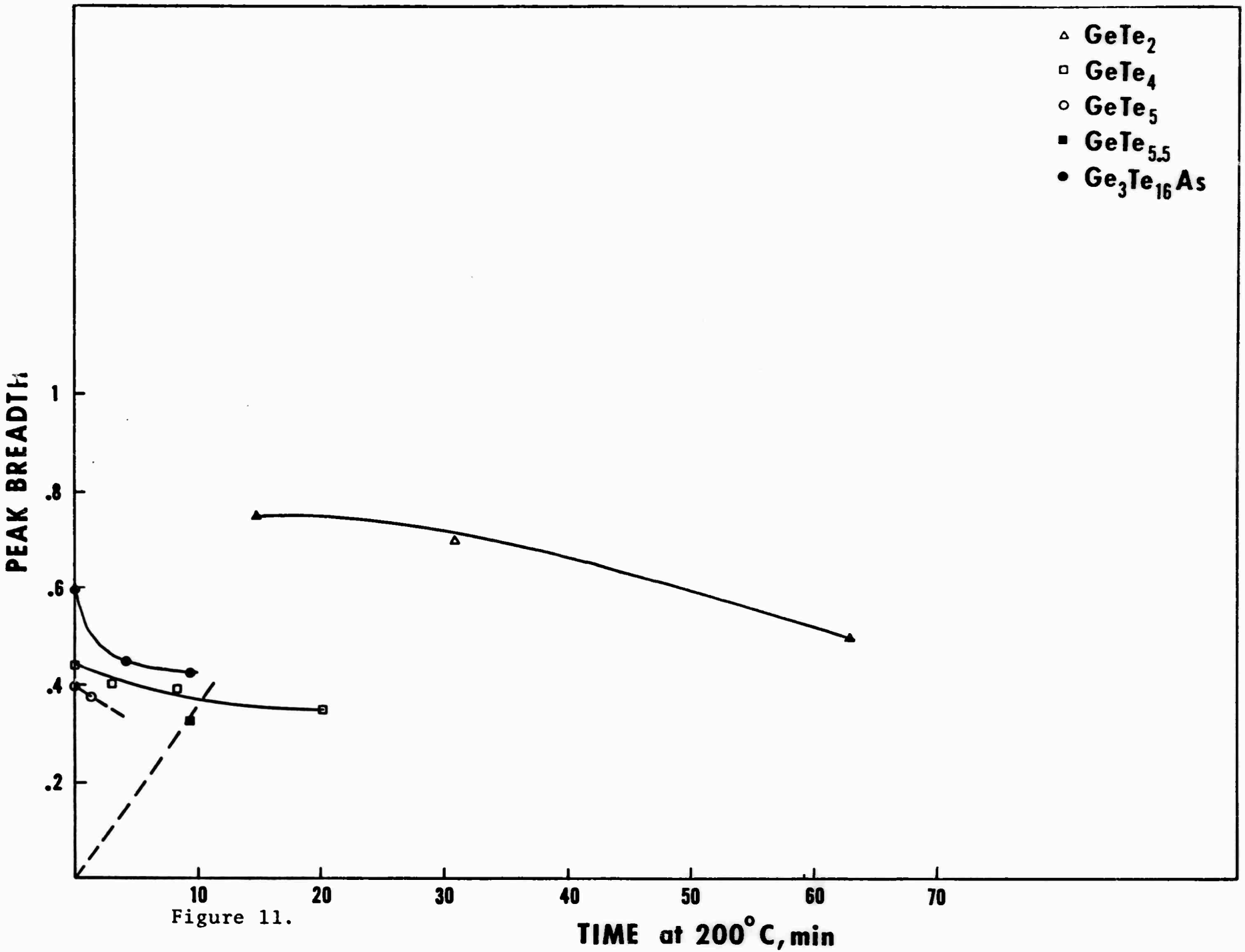
GeTe2
GeTe4
GeTe5
GeTe5.5
Ge3Te16As
PEAK BREADTH
1
.8
.6
.4
.2
10
20
30
40
50
60
70
TIME at 200°C, min

Figure 11.

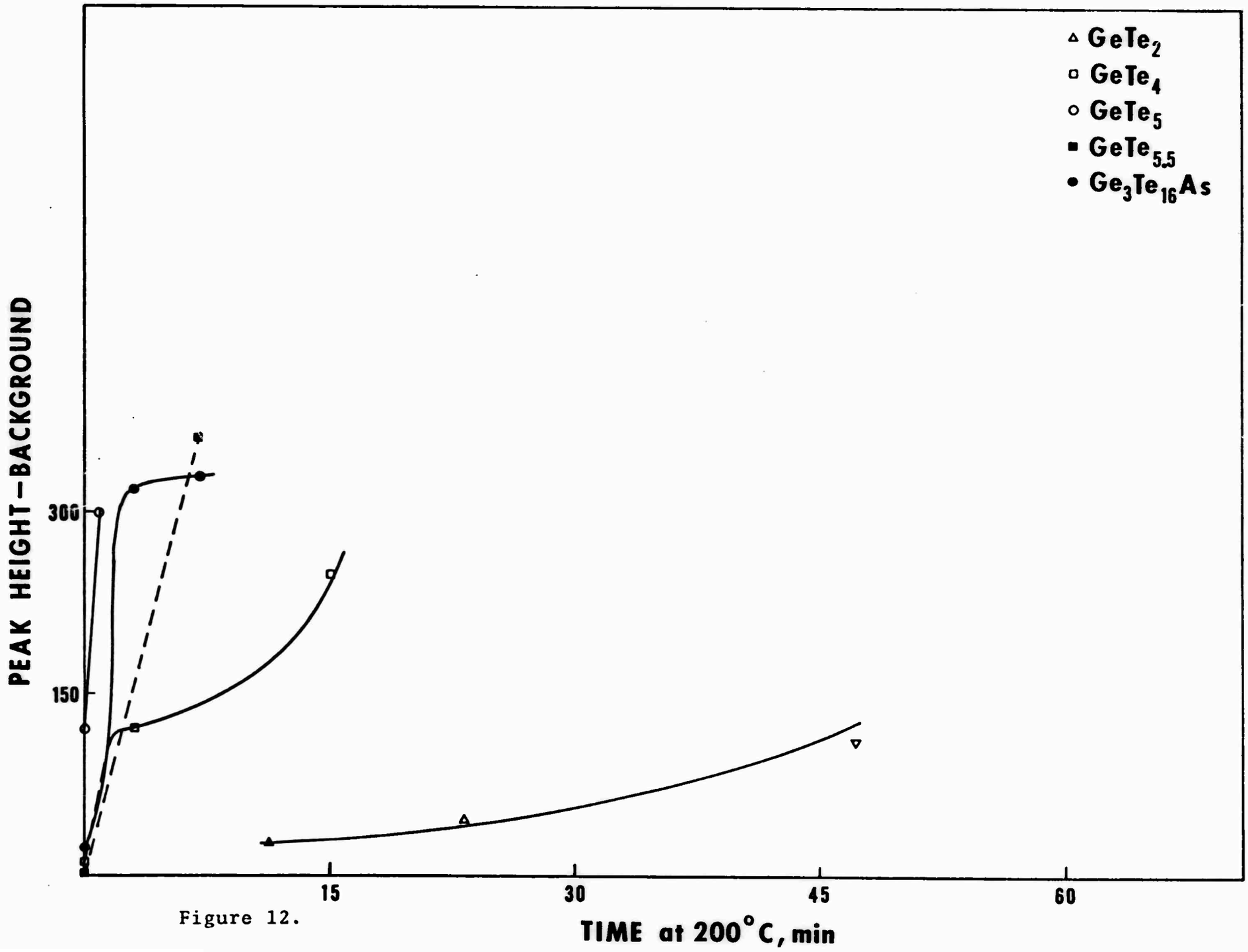
GeTe2
GeTe4
GeTe5
GeTe5.5
Ge3Te16As
PEAK HEIGHT–BACKGROUND
300
150
15
30
45
60
TIME at 200°C, min

Figure 12.

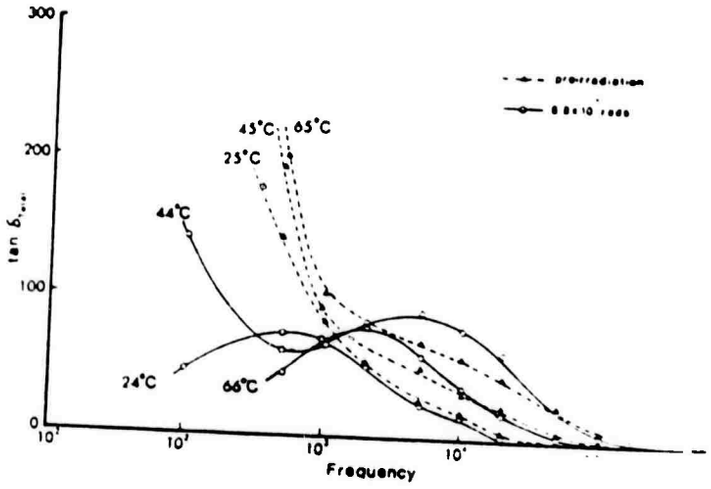

Figure 13.

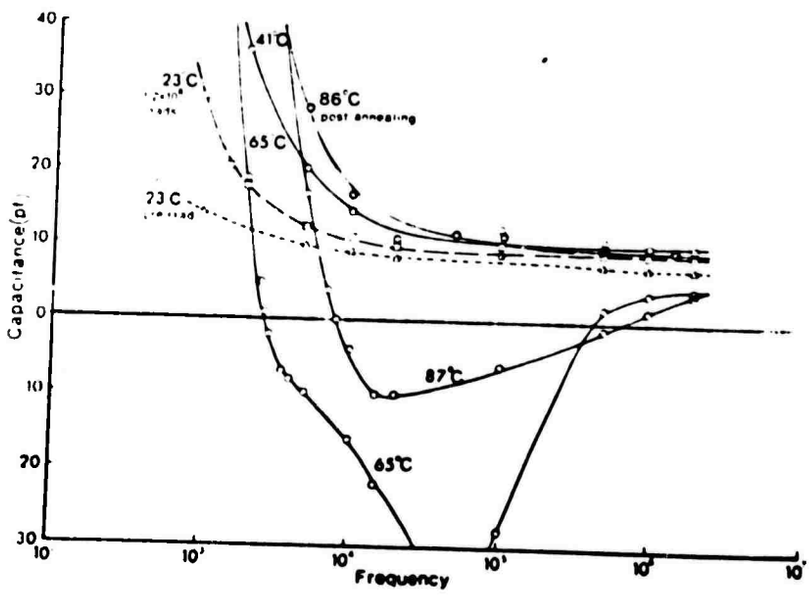

Figure 14.

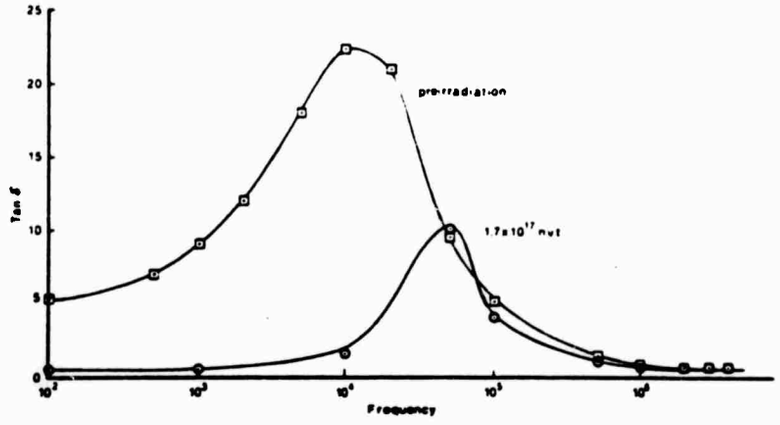
25
20
15
10
5
0
Tan δ
pre-irradiation
1.7x10^17 nvt
10^2
10^3
10^4
10^5
10^6
Frequency

Figure 15.

Unclassified

Security Classification

DOCUMENT CONTROL DATA - R & D

(Security classification of title, body of abstract and indexing annotation must be entered when the overall report is classified)

1. ORIGINATING ACTIVITY (Corporate author)
University of Florida, Engineering & Industrial Experiment Station, Gainesville, Florida 32601

2a. REPORT SECURITY CLASSIFICATION
Unclassified

2b. GROUP

3. REPORT TITLE
STRUCTURE, PROPERTIES AND RADIATION SENSITIVITY OF ELECTRICALLY BISTABLE MATERIALS

4. DESCRIPTIVE NOTES (Type of report and inclusive dates)
Technical Report, 1st Annual, 6 February 1970 to 6 February 1971

5. AUTHOR(S) (First name, middle initial, last name)
Derek B. Dove, Larry L. Hench, Robert W. Gould and Ronald E. Loehman

6. REPORT DATE	7a. TOTAL NO. OF PAGES	7b. NO OF REFS
6 February 1971	29	26

8a. CONTRACT OR GRANT NO
DAHC04-70-C-0024

b. PROJECT NO
P-8993-P

c.

d.

9a. ORIGINATOR'S REPORT NUMBER(S)
Technical Report No. 2

9b. OTHER REPORT NO(S) (Any other numbers that may be assigned this report)

10. DISTRIBUTION STATEMENT

11. SUPPLEMENTARY NOTES
This research was supported by Advanced Research Projects Agency

12. SPONSORING MILITARY ACTIVITY
Army Research Office, Durham

13. ABSTRACT

A range of semiconductors of compositions Ge_xSe_{1-x} and Ge_xTe_{1-x} have been prepared and have been examined by x-ray diffraction to verify the composition limits of the glass forming regions reported by previous workers. Thin films have been prepared by flash evaporation of crushed bulk compounds and have been subjected to rdf analysis and electron microscopy, and several structural models are compared. Studies on the crystallization kinetics of the glasses are being carried out with particular reference to material composition. An interpretation of these initial experiments is given in terms of a possible structural model for the glasses.

The importance of crystallite size on fast neutron damage threshold in heterogeneous amorphous semiconductors is emphasized and the results of radiation experiments on vanadage glasses are discussed.

DD FORM 1 NOV 65 1473

Security Classification

14 KEY WORDS	LINK A		LINK B		LINK C	
	ROLE	WT	ROLE	WT	ROLE	WT
amorphous semiconductors vanadate glasses radial distribution analysis thin film devices radiation effects						

END